

# 000 001 002 003 004 005 006 007 008 009 010 011 012 013 014 015 016 017 018 019 020 021 022 023 024 025 026 027 028 029 030 031 032 033 034 035 036 037 038 039 040 041 042 043 044 045 046 047 048 049 050 051 052 053 A BI-METRIC FRAMEWORK FOR EFFICIENT NEAREST NEIGHBOR SEARCH

Anonymous authors

Paper under double-blind review

## ABSTRACT

We propose a new “bi-metric” framework for designing nearest neighbor data structures. Our framework assumes two dissimilarity functions: a *ground-truth* metric that is accurate but expensive to compute, and a *proxy* metric that is cheaper but less accurate. In both theory and practice, we show how to construct data structures using only the proxy metric such that the query procedure achieves the accuracy of the expensive metric, while only using a limited number of calls to both metrics. Our theoretical results instantiate this framework for two popular nearest neighbor search algorithms: DiskANN and Cover Tree. In both cases we show that, as long as the proxy metric used to construct the data structure approximates the ground-truth metric up to a bounded factor, our data structure achieves arbitrarily good approximation guarantees with respect to the ground-truth metric. On the empirical side, we apply the framework to the text retrieval problem with two dissimilarity functions evaluated by ML models with vastly different computational costs. We observe that for almost all the large data sets in the BEIR benchmark, our approach achieves a considerably better accuracy-efficiency tradeoff than the alternatives, such as retrieve-then-rerank.

## 1 INTRODUCTION

Similarity search is a versatile and popular approach to data retrieval. It assumes that the data items of interest (text passages, images, etc.) are equipped with a distance function, which for any pair of items estimates their similarity or dissimilarity. Then, given a “query” item, the goal is to return the data item that is most similar to the query. From the algorithmic perspective, this approach is formalized as the nearest neighbor search (NN) problem: given a set of  $n$  points  $P$  in a metric space  $(X, D)$ , build a data structure that, given any query point  $q \in X$ , returns  $p \in P$  that minimizes  $D(p, q)$ . In many cases, the items are represented by high-dimensional feature vectors and  $D$  is induced by the Euclidean distance between the vectors. In other cases,  $D(p, q)$  is computed by a dedicated procedure given  $p$  and  $q$  (e.g., by a cross-encoder).

Over the last decade, mapping data items to feature vectors, or estimation of similarity between pairs of data items, is often done using ML models. (In the context of text retrieval, the first task is achieved by constructing bi-encoders (Karpukhin et al., 2020; Neelakantan et al., 2022; Gao et al., 2021b; Wang et al., 2024), while the second task uses cross-encoders (Gao et al., 2021a; Nogueira et al., 2020; Nogueira & Cho, 2020)). This creates efficiency bottlenecks, as high-accuracy models are often larger and slower, while cheaper models do not achieve the state-of-the-art accuracy. Furthermore, high-accuracy models are often proprietary and accessible only through a limited interface at a monetary cost. This motivates studying “the best of both worlds” solutions which utilize many types of models to achieve favorable tradeoffs between efficiency, accuracy and flexibility.

One popular method for combining multiple models is based on retrieve-then-rerank (Liu et al., 2009). It assumes two models: one model evaluating the metric  $D$ , which has high accuracy but is less efficient; and another model computing a “proxy” metric  $d$ , which is cheap but less accurate. The algorithm uses the second model ( $d$ ) to retrieve a large (say,  $k = 1000$ ) number of data items with the highest similarity to the query, and then uses the first model ( $D$ ) to select the most similar items. The hyperparameter  $k$  controls the tradeoff between the accuracy and efficiency. To improve the efficiency further, the retrieval of the top- $k$  items is typically accomplished using approximate

nearest neighbor data structures. Such data structures are constructed for the proxy metric  $d$ , so they remain stable even if the high-accuracy metric  $D$  undergoes frequent updates.

Despite its popularity, the retrieve-then-rerank approach suffers from several issues:

1. The overall accuracy is limited by the accuracy of the cheaper model. To illustrate this phenomenon, suppose that  $D$  defines the “true” distance, while  $d$  only provides a “ $C$ -approximate” distance, i.e., that the values of  $d$  and  $D$  for the same pairs of items differ by at most a factor of  $C > 1$ . Then the re-ranking approach can only guarantee that the top reported item is a  $C$ -approximation, namely that its distance to the query is at most  $C$  times the distance from the query to its true nearest neighbor according to  $D$ . This occurs because the first stage of the process, using the proxy  $d$ , might not retain the most relevant items.
2. Since the set of the top- $k$  items with respect to the more accurate model depends on the query, one needs to perform at least a linear scan over all  $k$  data items retrieved using the proxy metric  $d$ . This computational cost can be reduced by decreasing  $k$ , but at the price of reducing the accuracy.

**Our results** We show that, in both theory and practice, it is possible to combine cheap and expensive models to achieve approximate nearest neighbor data structures that inherit the accuracy of expensive models while significantly reducing the overall computational cost. Specifically, we propose a *bi-metric framework* for designing nearest neighbor data structures with the following properties: **(1)** The algorithm for creating the data structure uses only the proxy metric  $d$ , making it efficient to construct. **(2)** The algorithm for answering the nearest neighbor query leverages both models, but performs only a sub-linear number of evaluations of  $d$  and  $D$ . **(3)** The data structure achieves the accuracy of the expensive model.

For a more formal description of the framework, see Preliminaries (Section 2).

The simplest approach to constructing algorithms that conform to our framework is to *construct the data structure using the proxy metric  $d$ , but answer queries using the accurate metric  $D$* ; we also propose more complex solutions with better performance. Our approach is quite general, and is applicable to any approximate nearest neighbor data structure for general metrics. Our *theoretical* study analyzes the simple approach when applied to two popular algorithms: DiskANN (Jayaram Subramanya et al., 2019) and Cover Tree (Beygelzimer et al., 2006), under natural assumptions about the intrinsic dimensionality of the data, as in Indyk & Xu (2023). Perhaps surprisingly, we show that despite the fact that only the proxy  $d$  is used in the indexing stage, the query answering procedure essentially retains the accuracy of the ground truth metric  $D$ .

Formally, we show the following theorem statement. We use  $\lambda_d$  to refer to the doubling dimension with respect to metric  $d$  (a measure of intrinsic dimensionality, see Definition 2.2).

**Theorem 1.1** (Summary, see Theorems 3.3 and B.3). *Given a dataset  $X$  of  $n$  points,  $\text{Alg} \in \{\text{DiskANN}, \text{Cover Tree}\}$ , and a fixed metric  $d$ , let  $S_{\text{Alg}}(n, \varepsilon, \lambda_d)$  and  $Q_{\text{Alg}}(\varepsilon, \lambda_d)$  denote the space and query complexity respectively of the standard datastructure for  $\text{Alg}$  which reports a  $1 + \varepsilon$  nearest neighbor in  $X$  for any query (all for a fixed metric  $d$ ).*

*Consider two metrics  $d$  and  $D$  satisfying Equation 1. Then for any  $\text{Alg} \in \{\text{DiskANN}, \text{Cover Tree}\}$ , we can build a corresponding datastructure  $\mathcal{D}_{\text{Alg}}$  on  $X$  with the following properties:*

1. *When constructing  $\mathcal{D}_{\text{Alg}}$ , we only access metric  $d$ ,*
2. *The space used by  $\mathcal{D}_{\text{Alg}}$  can be bounded by  $\tilde{O}(S_{\text{Alg}}(n, \varepsilon/C, \lambda_d))^1$ ,*
3. *Given any query  $q$ ,  $\mathcal{D}_{\text{Alg}}$  invokes  $D$  at most  $\tilde{O}(Q_{\text{Alg}}(\varepsilon/C, \lambda_d))$  times,*
4.  *$\mathcal{D}_{\text{Alg}}$  returns a  $1 + \varepsilon$  approximate nearest neighbor of  $q$  in  $X$  under metric  $D$ .*

The proof of the theorem crucially uses the properties of the underlying graph-based data structures. In Appendix F, we theoretically show that such a result is impossible to achieve for another popular family of nearest neighbor algorithms based on *locality sensitive hashing* (and other similar methods). Thus our work further highlights the *power* of graph-based methods, both theoretically and empirically.

To demonstrate the *practical* applicability of the bi-metric framework, we apply it to the text retrieval problem. Here, the data items are text passages, and the goal is to retrieve a passage from a large

<sup>1</sup> $\tilde{O}$  hides logarithm dependencies in the aspect ratio.

108 collection that is most relevant to a query passage. We instantiated our framework with the DiskANN  
 109 algorithm. We use a lower-quality “bge-micro-v2” embedding model (AI, 2023) to define the metric  
 110  $d$ ; the value of  $d(p, q)$  is defined by the Euclidean distance between the embeddings of  $p$  and  $q$ . The  
 111 high-quality model  $D$  is defined by one of the following two settings: **(1)** The *SFR-Embedding*-  
 112 *Mistral* embedding model (Meng et al., 2024), where the metric is defined as the Euclidean distance  
 113 between embeddings, and **(2)** The *Gemini-2.0-Flash* large language model. Here, we use the fact that  
 114 graph-based algorithms for nearest neighbor search do not require the values  $D(p, q)$  per se, but only  
 115 use comparisons between  $D(q, p)$  and  $D(q, s)$ . We implement these comparisons by querying the  
 116 model with a query  $q$  and a list of points  $\{p_1, p_2, \dots, p_n\}$  to obtain their relative order via the model  
 117 API, where the list of points is generated by our algorithm. Please refer to Algorithm 4 in Appendix  
 118 for details.

119 In all the cases, the complexities of the high-quality model are much higher than that of the low-  
 120 quality model. In the first setting, embedding a single passage takes 0.00043 seconds when using  
 121 bge-micro-v2 compared to 0.13 seconds when using SFR-Embedding-Mistral, making the second  
 122 model **>300** times slower. In the second setting, bge-micro-v2 embeddings are computed locally,  
 123 while the comparisons involving the high-quality metric require calls to Gemini-2.0-Flash API, at a  
 124 cost of roughly 0.01 cents per distance evaluation, amounting to a total of \$1000 to reproduce the  
 125 experimental results in Figure 2.

126 We evaluated the retrieval quality of our approach on a benchmark collection of 6 large (i.e., of size  
 127  $\geq$  one million) BEIR retrieval data sets Thakur et al. (2021). In each experiment we compared our  
 128 algorithm to the standard the re-ranking approach, which retrieves the closest data items to the query  
 129 with respect to  $d$  and re-ranks using  $D$ . We observe that in almost all settings, our approach achieves  
 130 a considerably better accuracy-efficiency tradeoff than re-ranking. For example, in Gemini-2.0-Flash  
 131 experiments, on average, our algorithm achieves the same retrieval accuracy as re-ranking using only  
 132  $\approx 200$  calls to the Gemini API, compared with  $\approx 800$  calls by re-ranking, a **4x** reduction (Figure 2).

133

134 **Related Work** As described in the introduction, a popular method for utilizing a cheap metric  $d$   
 135 and expensive metric  $D$  in similarity search is based on “filtering” or “re-ranking”. The idea is to  
 136 use  $d$  to construct a (long) list of candidate answers, which is then filtered using  $D$  (Matveeva et al.,  
 137 2006). It is a popular approach in many applications, including recommendation systems (Liu et al.,  
 138 2022) and computer vision (Zhong et al., 2017). Due to the popularity of this method, we use it as a  
 139 baseline in our experiments.

140 In addition to the re-ranking method, multiple other papers proposed different methods for combining  
 141 accurate and cheap metrics to improve similarity search and related problems. We discuss those  
 142 papers in more detail below. We note that, with the exception of Moseley et al. (2021); Silwal et al.  
 143 (2023); Bateni et al. (2024), those methods do not appear to come with provable correctness or  
 144 efficiency guarantees, or generally applicable frameworks (in contrast to the proposal in this paper).  
 145 Furthermore, the three aforementioned papers (Moseley et al., 2021; Silwal et al., 2023; Bateni et al.,  
 146 2024) focus on various forms of clustering, not on similarity search. The paper Moseley et al. (2021)  
 147 is closest to our work, as it uses approximate nearest neighbor as a subroutine when computing the  
 148 clustering. However, their algorithm only achieves the (lower) accuracy of the cheaper model, while  
 149 our algorithms retains the (higher) accuracy of the expensive one.

150 There are also several other empirical works on similarity search that combine cheap and expensive  
 151 metrics, none of which fully capture our framework to the best of our knowledge. The aforementioned  
 152 paper Jayaram Subramanya et al. (2023) describes (in section 3.1) an optimization which uses  
 153 the ground truth metric  $D$  during the indexing phase, and proxy metric  $d$ , obtained via product  
 154 quantization Jegou et al. (2010) during the search phase. In contrast, our framework uses  $D$  during  
 155 the *search phase* and  $d$  during *indexing*. This difference seems crucial to our ability of providing  
 156 strong approximation guarantees for the reported points. In another paper Chen et al. (2023), the  
 157 authors use the proxy metric  $d$  obtained by “sketching”  $D$  during the query answering phase, in order  
 158 to prune some points from the search queue without resorting to computing  $D$ . However, the data  
 159 structure index is still constructed using the expensive metric  $D$ , as opposed the proxy metric  $d$  as  
 160 in our framework, which makes preprocessing more expensive in terms of space and time. Finally,  
 161 Morozov & Babenko (2019) present a method for constructing a similarity graph with respect to  
 an approximate distance function derived from a complex one; during the query phase the graph is  
 explored using a more complex relevance function. However, their algorithm uses specific proxy

metric derived from the expensive one; in contrast, our framework allows arbitrary distance functions  $d$  and  $D$ , as long as the distortion  $C$  between them is bounded. We discuss further related work pertaining to graph-based algorithms for similarity search in Appendix A.

## 2 PRELIMINARIES

**Nearest neighbor search** We first consider the standard formulation of *exact* nearest neighbor search. Here, we are given a set of points  $P$ , which is a subset of the set of all points  $X$  (e.g.,  $X = \mathbb{R}^{\text{dim}}$ ). In addition, we are given access to a metric function  $D$  that, for any pair of points  $p, q \in X$  returns the dissimilarity between  $p$  and  $q$ . The goal of the problem is to build an index structure that, given a *query* point  $q \in X$ , returns  $p^* \in P$  such that  $p^* = \arg \min_{p \in P} D(q, p)$ . The formulation is naturally extended to more general settings, such as:

- $(1 + \varepsilon)$ -approximate nearest neighbor search, where the goal is to find any  $p^* \in P$  such that  $D(q, p^*) \leq (1 + \varepsilon) \min_{p \in P} D(q, p)$ .
- $k$ -nearest neighbor search, where the goal is to find the set of  $k$  nearest neighbors of  $q$  in  $P$  with respect to  $D$ . If the algorithm returns a set  $S'$  of size  $k$  different than the set  $S$  of true  $k$  nearest neighbor, the answer quality is measured via Recall or NDCG score (Järvelin & Kekäläinen, 2002).

### Bi-metric framework

In our framework, we assume that we are given *two* metrics over  $X$ :

- The *ground truth* metric  $D$ , which for any pair of points  $p, q \in X$  returns the “true” dissimilarity between  $p$  and  $q$ . The metric  $D$  plays the same role as in the standard nearest neighbor search problem.
- The *proxy* metric  $d$ , which provides a cheap approximation to the ground truth metric.

**Objective:** return nearest neighbors with respect to the expensive metric  $D$ ; the metric  $d$  is used as a proxy, in order to minimize the number of calls to the expensive metric  $D$ .

**Cost model:** We assume that the algorithm for constructing the data structure can use the proxy metric  $d$ , but *not* the ground truth metric  $D$ . On the other hand, the algorithm for answering a query  $q$  has access to *both* metrics. However, the complexity of the query-answering procedure is measured by counting only the number of evaluations of the expensive metric  $D$ .

As described in the introduction, the above formulation is motivated by the following considerations:

- In many scenarios, evaluating the ground truth metric  $D$  can be very expensive, due to factors such as model size or monetary costs associated with querying proprietary models from industry. For example, a typical call to Gemini-2.0-Flash costs roughly 0.01 cents per distance evaluation. For SFR-Embedding-Mistral (Meng et al., 2024), it takes an A100 gpu around 196 hours to compute the embeddings of 5 million passages from the HotpotQA dataset and these embeddings occupy 83GB of disk storage; meanwhile, using the cheap model bge-micro (AI, 2023), computing these embeddings only takes 0.62 hours and 7GB of disk storage. (As a comparison, the graph index size of 5 million points occupies roughly 1GB of disk storage.) Therefore, our cost model for the query answering procedure only accounts for the number of expensive evaluations.
- In other settings, a cheap proxy metric  $d$  can be obtained by approximating the ground truth metric  $D$ , i.e., by using product quantization (Jegou et al., 2010).
- In applications that use similarity search data structures in model training, the metric  $D$  can change after each model update, necessitating re-computing embeddings and the search index over the entire database. Since this is expensive, some works (e.g., Borgeaud et al. (2022)) freeze the parts of the model that compute embeddings to avoid the computational cost of updating the data structure. Our framework offers an alternative approach, where one constructs a stable index for a proxy  $d$  using frozen embeddings, but uses the up-to-date model to compute the ground-truth metric  $D$  when answering nearest neighbor queries.

216 **Design approach:** On a high-level, the algorithms studied in this paper follow the same design  
 217 pattern. Specifically, we use a graph-based nearest neighbor search algorithm, which uses calls to  
 218 a metric as a black box, as a starting point. During preprocessing, the algorithm uses the proxy  
 219 metric  $d$ . However, during the query phase, the algorithm makes calls to the accurate metric  $D$ . We  
 220 show that, despite this “metric switch”, the resulting algorithm can report provably accurate nearest  
 221 neighbors with respect to the accurate metric  $D$ . This basic approach is then modified to achieve better  
 222 performance, in theory and in practice. We apply this design approach to two popular graph-based  
 223 algorithms: DiskANN and Cover Tree, but in principle any other graph-based algorithm can also  
 224 be used. (We choose these two algorithms because both have provable correctness & performance  
 225 guarantees, making it possible for us to obtain provable guarantees for our methods as well.)  
 226

227 **Assumptions about metrics:** Clearly, if the metrics  $d$  and  $D$  are not related to each other, the data  
 228 structure constructed using  $d$  alone does not help with the query retrieval. Therefore, we assume that  
 229 the two metrics are related through the following definition.

230 **Definition 2.1.** Distance function  $d$  is a  $C$ -approximation<sup>2</sup> of  $D$  if for all  $x, y \in X$ ,  $d(x, y) \leq$   
 231  $D(x, y) \leq C \cdot d(x, y)$ . (1)

232 For a fixed metric  $d$  and any point  $p \in X$ , radius  $r > 0$ , we use  $B(p, r)$  to denote the ball with radius  
 233  $r$  centered at  $p$ , i.e.  $B(p, r) = \{q \in X : d(p, q) \leq r\}$ . In our paper, the notion of *doubling-dimension*  
 234 is central. It is a measure of intrinsic dimensionality of datasets which is popular in analyzing high  
 235 dimensional datasets, especially in the context of nearest neighbor search algorithms (Gupta et al.,  
 236 2003; Krauthgamer & Lee, 2004a;b; Beygelzimer et al., 2006; Indyk & Naor, 2007; Har-Peled &  
 237 Kumar, 2013; Narayanan et al., 2021; Indyk & Xu, 2023). Furthermore, it is known Krauthgamer &  
 238 Lee (2004b) that the complexity of approximate nearest neighbor algorithms that work for general  
 239 metrics must depend the doubling dimension.

240 **Definition 2.2 (Doubling Dimension).**  $X$  has doubling dimension  $\lambda_d$  with respect to metric  $d$  if for  
 241 any  $p \in X$ , and radius  $r > 0$ ,  $X \cap B(p, 2r)$  can be covered by at most  $2^{\lambda_d}$  balls with radius  $r$ .  
 242

243 For a metric  $d$ ,  $\Delta_d$  is the *aspect ratio* of the input set, i.e.,  $\Delta_d = \text{Diam}_d / C_d$ , where  $\text{Diam}_d$  is the  
 244 maximum distance between any pairs of points under  $d$ , and  $C_d$  is the distance between the pair of  
 245 closest distinct points under  $d$ . Note that both Definition 2.1 and 2.2 are only used in our theoretical  
 246 analysis. Our experimental results verify that the algorithms inspired by our bi-metric framework can  
 247 yield performance speedups *without any assumptions*; see Section 4.

### 249 3 THEORETICAL ANALYSIS

250 We instantiate our *bi-metric* framework for two popular nearest neighbor search algorithms: DiskANN  
 251 and Cover Tree. We note that, if we treat the proxy data structure as a *black box*, we can only guarantee  
 252 that it returns a  $C$ -approximate nearest neighbor with respect to  $D$ . Our theoretical analysis overcomes  
 253 this, and shows that calling  $D$  a sublinear number of times in the query phase (for DiskANN and  
 254 Cover Tree) allows us to obtain *arbitrarily accurate* neighbors for  $D$ .

255 At a high level, the unifying theme of the algorithms that we analyze is that they both crucially use  
 256 the concept of a *net*: given a parameter  $r$ , a  $r$ -net is a small subset of the dataset guaranteeing that  
 257 every data point is within distance  $r$  to the subset in the net. Both algorithms (implicitly or explicitly),  
 258 construct nets of various scales  $r$  which help route queries to their nearest neighbors in the dataset.  
 259 The key insight is that a net of scale  $r$  for metric  $d$  is also a net under metric  $D$ , but with the larger  
 260 scale  $Cr$ . Thus, if we construct smaller nets for metric  $d$ , they can also function as nets for the  
 261 expensive metric  $D$ . Theoretically, this is where the advantage of our method comes from, but care  
 262 must be taken to formalize the intuition.

263 We remark that the intuition we gave clearly does not generalize for nearest neighbor algorithms  
 264 which are fundamentally different, such as locality sensitive hashing. In fact, in Appendix F we  
 265 *theoretically show that such a result is impossible to achieve for LSH*. We present the analysis of  
 266 DiskANN below. The analysis of Cover Tree is more complex, and hence deferred to Appendix B.  
 267

268  
 269 <sup>2</sup>Please see Section 4 and Figure 6 for empirical estimates of  $C = D/d$ . For all datasets,  $C = O(1)$  for  
 most pairs, justifying the use of this assumption.

270 **Preliminaries for DiskANN.** First, some helpful background is given. First we only deal with  
 271 a single metric  $d$ . We first need the notion of an  $\alpha$ -shortcut reachability graph. Intuitively, it is an  
 272 unweighted graph  $G$  where the vertices correspond to points of a dataset  $X$  such that nearby points  
 273 (geometrically) are close in graph distance. The main analysis of Indyk & Xu (2023) shows that (the  
 274 ‘slow preprocessing version’ of ) DiskANN outputs an  $\alpha$ -shortcut reachability graph (Theorem A.1).

275 **Definition 3.1** ( $\alpha$ -shortcut reachability Indyk & Xu (2023)). Let  $\alpha \geq 1$ . We say a graph  $G = (X, E)$   
 276 is  $\alpha$ -shortcut reachable from a vertex  $p$  under a given metric  $d$  if for any other vertex  $q$ , either  
 277  $(p, q) \in E$ , or there exists  $p'$  s.t.  $(p, p') \in E$  and  $d(p', q) \cdot \alpha \leq d(p, q)$ . We say a graph  $G$  is  
 278  $\alpha$ -shortcut reachable under metric  $d$  if  $G$  is  $\alpha$ -shortcut reachable from any vertex  $v \in X$ .

279 Given an  $\alpha$ -reachability graph on dataset  $X$  and a query  $q$ , Indyk & Xu (2023) show that the greedy  
 280 search procedure of Algorithm 1 (given in Appendix A) finds accurate nearest neighbor of  $q$  in  $X$ .

282 **Theorem 3.2** ( Indyk & Xu (2023)). For  $\varepsilon \in (0, 1)$ , there exists an  $\Omega(1/\varepsilon)$ -shortcut reachable graph  
 283 index for a metric  $d$  with max degree  $\text{Deg} \leq (1/\varepsilon)^{O(\lambda_d)} \log(\Delta_d)$  (guaranteed by Theorem A.1). For  
 284 any query  $q$ , Algorithm 1 on this graph index finds a  $(1 + \varepsilon)$  nearest neighbor of  $q$  in  $X$  (under metric  
 285  $d$ ) in  $S \leq O(\log(\Delta_d))$  steps and makes at most  $S \cdot \text{Deg} \leq (1/\varepsilon)^{O(\lambda_d)} \log(\Delta_d)^2$  calls to  $d$ .

286 We are now ready to state the main theorem of this section.

288 **Theorem 3.3.** Let  $Q_{\text{DiskAnn}}(\varepsilon, \Delta_d, \lambda_d) = (1/\varepsilon)^{O(\lambda_d)} \log(\Delta_d)^2$  denote the query complexity of the  
 289 DiskANN data structure<sup>3</sup>, where we build and search using the same metric  $d$ . Consider two metrics  $d$   
 290 and  $D$  satisfying Equation 1. Suppose we build an  $C/\varepsilon$ -shortcut reachability graph  $G$  using Theorem  
 291 A.1 for metric  $d$ , but search using metric  $D$  in Algorithm 1 for a query  $q$  with  $L = 1$ . Then:

292 1. The space used by  $G$  is at most  $n \cdot (C/\varepsilon)^{O(\lambda_d)} \log(\Delta_d)$ .  
 293 2. Running Algorithm 1 using  $D$  finds a  $1 + \varepsilon$  nearest neighbor of  $q$  in the dataset  $X$  (under  $D$ ).  
 294 3. On any query  $q$ , Algorithm 1 invokes  $D$  at most  $Q_{\text{DiskAnn}}(\varepsilon/C, C\Delta_d, \lambda_d)$ .

296 To prove the theorem, we first show that a shortcut reachability graph of  $d$  is also a shortcut reachability  
 297 graph of  $D$ , albeit with slightly different parameters, with a proof in Appendix C.

299 **Lemma 3.4.** Suppose metrics  $d$  and  $D$  satisfy relation (1). Suppose  $G = (X, E)$  is  $\alpha$ -shortcut  
 300 reachable under  $d$  for  $\alpha > C$ . Then  $G = (X, E)$  is an  $\alpha/C$ -shortcut reachable under  $D$ .

301 *Proof of Theorem 3.3.* By Lemma 3.4, the graph  $G = (X, E)$  constructed for metric  $d$  is also  
 302 a  $O(1/\varepsilon)$  reachable for the other metric  $D$ . Then we simply invoke Theorem 3.2 for a  $(1/\varepsilon)$ -  
 303 reachable graph index for metric  $D$  with degree limit  $\text{Deg} \leq (C/\varepsilon)^{O(\lambda_d)} \log(\Delta_d)$  and the number  
 304 of greedy search steps  $S \leq O(\log(C\Delta_d))$ . Thus the total number of  $D$  distance call bounded by  
 305  $(C/\varepsilon)^{O(\lambda_d)} \log(C\Delta_d)^2 \leq Q_{\text{DiskAnn}}(\varepsilon/C, C\Delta_d, \lambda_d)$ . This proves the accuracy bound as well as the  
 306 number of calls we make to metric  $D$  during the greedy search procedure of Algorithm 1. The space  
 307 bound follows from Theorem A.1, since  $G$  is a  $C/\varepsilon$ -reachability graph for metric  $d$ .  $\square$

## 309 4 EXPERIMENTS

311 The starting point of our implementation is the DiskANN based algorithm from Theorem 3.3, which  
 312 we engineer to optimize performance<sup>4</sup>. We compare it to two other methods on all large BEIR  
 313 retrieval tasks (Thakur et al., 2021), i.e., for datasets with corpus size  $> 10^6$ , see below.

315 **Methods** We evaluate the following methods.  $Q$  denotes the query budget, i.e., the maximum number  
 316 of calls an algorithm can make to  $D$  during a query. We vary  $Q$  in our experiments.

317 • Bi-metric (our method): We build a graph index with the cheap distance function  $d$  (we discuss our  
 318 choice of graph indices in the experiments shortly). Given a query  $q$ , we first search for  $q$ ’s top- $Q/2$   
 319 nearest neighbor under metric  $d$ . Then, we start a second-stage search from the  $Q/2$  returned vertices  
 320 using distance function  $D$  on the same graph index until we reach the quota  $Q$ . We report the 10  
 321 closest neighbors seen so far by distance function  $D$ .

322 <sup>3</sup>I.e., the upper bound on the number of calls made to  $d$  on any query

323 <sup>4</sup>Our experiments are run on 56 AMD EPYC-Rome processors with 400GB of memory and 4 NVIDIA RTX  
 6000 GPUs. Our experiment in Figure 1 takes roughly 3 days.

324 • **Bi-metric (baseline):** This is the standard retrieve-then-rerank method that is widely popular. We  
 325 build a graph index with the cheap distance function  $d$ . Given a query  $q$ , we first search for  $q$ 's top- $Q$   
 326 nearest neighbor under metric  $d$ . As explained below, we can assume that empirically the first step  
 327 returns the *true* top- $Q$  nearest neighbors under  $d$ . Then, we calculate distance using  $D$  for all the  $Q$   
 328 returned vertices and report the top-10.

329 • **Single metric:** This is the standard nearest neighbor search with a single distance function  $D$ . We  
 330 build the graph index directly with the expensive distance function  $D$ . Given a query  $q$ , we do a  
 331 standard greedy search to get the top-10 closest vertices to  $q$  with respect to distance  $D$  until we reach  
 332 quota  $Q$ . We ignore the large number of  $D$  distance calls in the indexing phase and only count the  
 333 quota in the search phase. Note that this method doesn't satisfy our "bi-metric" formulation as it uses  
 334 an extensive number of  $D$  distance calls ( $\Omega(n)$  calls) in index construction. However, we implement  
 335 it for comparison since it represents a natural baseline, if one does not care about the prohibitively  
 336 large number of calls made to  $D$  during index building.

337 For both Bi-metric methods (ours and baseline), in the first-stage search under distance  $d$ , we  
 338 initialize the parameters of the graph index so that empirically, it returns the true nearest neighbors  
 339 under distance  $d$ . This is done by setting the 'queue length' parameter  $L$  to be 30000 for datasets  
 340 with corpus size  $> 10^6$  (Climate-FEVER (Diggelmann et al., 2020), FEVER (Thorne et al., 2018),  
 341 HotpotQA (Yang et al., 2018), MSMARCO (Bajaj et al., 2018), NQ (Kwiatkowski et al., 2019),  
 342 DBpedia (Hasibi et al., 2017)). Our choice of  $L$  is large enough to ensure that the returned vertices  
 343 are almost true nearest neighbors under distance  $d$ . For example, the standard parameters used are a  
 344 factor of 10 smaller. We also empirically verified that the nearest neighbors returned for  $d$  with such  
 345 large values of  $L$  corroborated with published BEIR benchmark values<sup>5</sup>.

346 **Datasets** We experiment with all 6 BEIR retrieval datasets of size  $> 10^6$  (Climate-FEVER (Diggel-  
 347 mann et al., 2020), FEVER (Thorne et al., 2018), HotpotQA (Yang et al., 2018), MSMARCO (Bajaj  
 348 et al., 2018), NQ (Kwiatkowski et al., 2019), DBpedia (Hasibi et al., 2017)). We report the results on  
 349 these datasets' test split, except for MSMARCO where we report the results on its dev split.

350 **Embedding Models** We select a highly ranked model "SFR-Embedding-Mistral" as our expensive  
 351 model to provide groundtruth metric  $D$ . Meanwhile, we select three models on the pareto curve of the  
 352 BEIR retrieval size-average score plot to test how our method performs under different model scale  
 353 combinations. These three small models are "bge-micro-v2", "gte-small", "bge-base-en-v1.5". Please  
 354 refer to Table 1 for details. As described earlier, both metrics  $d(p, q)$  and  $D(p, q)$  are induced by the  
 355 Euclidean distance between the embeddings of  $p$  and  $q$  using the respective models. The embeddings  
 356 defining the proxy metric  $d$  are pre-computed and stored during the pre-processing, and then used to  
 357 construct the data structure. The embeddings defining the accurate metric  $D$  are computed on the fly  
 358 during the query processing stage. Specifically, to answer a query  $q$ , the algorithm first computes the  
 359 embedding  $f(q)$  of  $q$ . Then, whenever the value of  $D(q, p)$  is needed, the algorithm computes  $f(p)$   
 360 and evaluates  $D(p, q) = \|f(q) - f(p)\|$ . Thus, the cost of evaluating  $D(p, q)$  is equal to the cost of  
 361 embedding  $p$ . (In other scenarios where  $D(p, q)$  is evaluated using a proprietary system over an API  
 362 call, the cost is determined by the vendor's prices and/or the network speed.).

Model Name	Embedding Dimension	Model Size	BEIR Retrieval Score
SFR-Embedding-Mistral (Meng et al., 2024)	4096	7111M	59
bge-base-en-v1.5 (Xiao et al., 2023)	768	109M	53.25
gte-small (Li et al., 2023)	384	33M	49.46
bge-micro-v2 (AI, 2023)	384	17M	42.56

368 Table 1: Different models used in our experiments

369 **Nearest Neighbor Search Algorithms** The search algorithms we employ in our experiments are  
 370 DiskANN (Jayaram Subramanya et al., 2019) and NSG (Fu et al., 2019a). We use standard parameter  
 371 choices for both; see Appendix E.

373 **Metric** Given a fixed expensive distance function quota  $Q$ , we report the accuracy of retrieved results  
 374 for different methods. We always insure that all algorithms never use more than  $Q$  expensive distance  
 375 computations. Following the BEIR retrieval benchmark, we report the NDCG@10 score. In addition,  
 376 we also report Recall@10, where the ground truth is defined by the 10 nearest neighbors according

377 <sup>5</sup>from <https://huggingface.co/spaces/mteb/leaderboard>

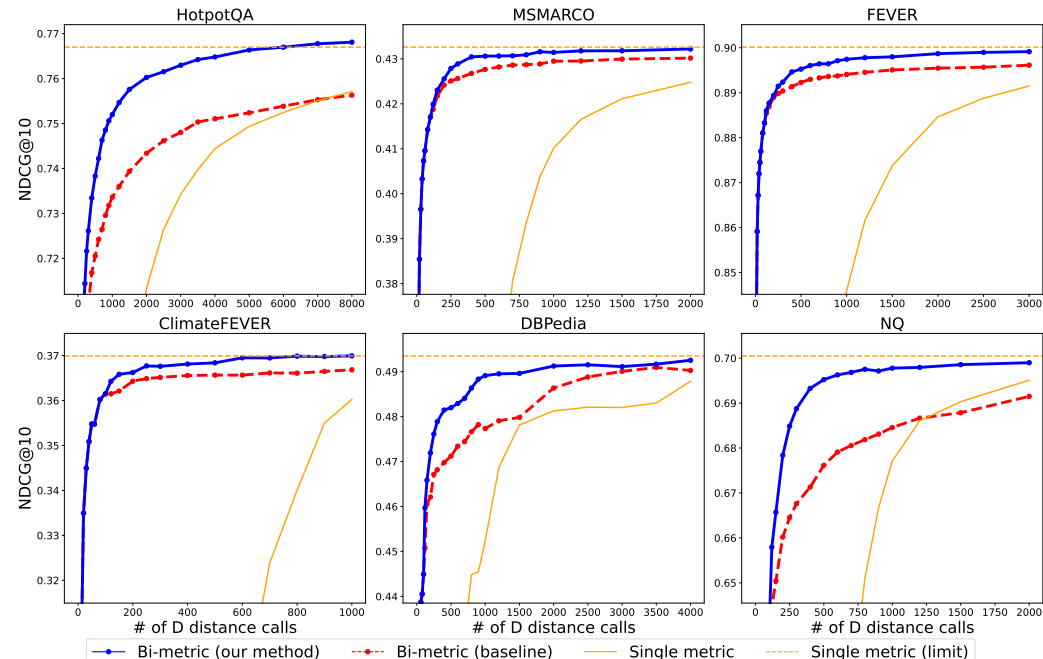
378 to the expensive metric  $D$ ; this is akin to the methodology used to evaluate approximate nearest  
 379 neighbor search algorithms.  
 380

#### 381 4.1 EXPERIMENT RESULTS AND ANALYSIS 382

383 Please refer to Figure 1 for our results with  $d$  distance function set to “bge-micro-v2” and  $D$  set to  
 384 “SFR-Embedding-Mistral”, with the underlying graph index being DiskANN. To better focus on the  
 385 convergence speed of different methods toward the “Single metric (limit)” (perfect nearest neighbor  
 386 retrieval with respect to  $D$ ), we cut off the y-axis at a relatively high accuracy, so some curves may  
 387 not start from x equals 0 if their accuracy doesn’t reach the threshold. We observe that our method  
 388 converges to the optimal accuracy much faster than bi-metric (baseline) and single metric in most  
 389 cases. For example for HotpotQA, the NDCG@10 score achieved by the baselines for 8000 calls to  
 390  $D$  is comparable to our method, using less than 2000 calls to  $D$ , leading to  $> 4x$  fewer evaluations of  
 391 the expensive model. This leads to substantial time savings. For example, consider our largest data  
 392 set HotpotQA. The first stage of the query answering procedure (using  $d$ ) takes only 0.37s per query  
 393  $q$ , while each evaluation of  $D(p, q)$  during the second stage takes 0.13s; this translates into roughly  
 394 260s per query when 2000 evaluations of  $D$  are used. In contrast, the baseline method requires 8000  
 395 calls to  $D$ , which translates into a cost of roughly 1040s per query.  
 396

397 This means that utilizing the graph index built for the distance function proxy to perform a greedy  
 398 search using  $D$  is more efficient than naively iterating the returned vertex list to re-rank using  $D$   
 399 (baseline). Also note that our method converges faster than “Single metric” in all the datasets. This  
 400 phenomenon happens even if “Single metric” is allowed infinite expensive distance function calls  
 401 in its indexing phase to build the ground truth graph index. This suggests that the quality of the  
 402 underlying graph index is not as important, and the early routing steps in the searching algorithm can  
 403 be guided with a cheap distance proxy functions to save expensive distance function calls.  
 404

405 Similar conclusion holds for the recall plot (see Figure 7), where our method has an even larger  
 406 advantage over Bi-metric (baseline) and is better than the Single metric in most cases, except FEVER  
 407 and HotpotQA. We report the results of using different model pairs, using the NSG algorithm as our  
 408 graph index, and measuring Recall@10 in Appendix E. Please see ablation studies in Appendix D.  
 409



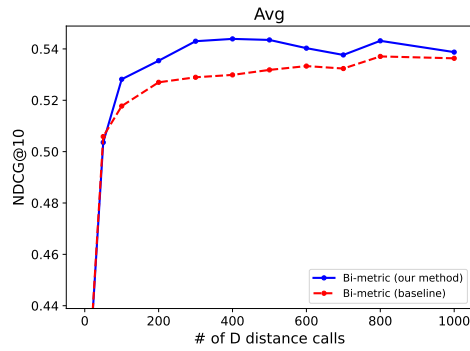
410  
 411 Figure 1: Results for 6 BEIR Retrieval datasets. The x-axis is the number of expensive distance  
 412 function calls. The y-axis is the NDCG@10 score. The cheap model is “bge-micro-v2”, the expensive  
 413 model is “SFR-Embedding-Mistral”, and the nearest neighbor search algorithm used is DiskANN.  
 414

415 Lastly, we measure the empirical value of  $C$  (the relationship between  $d/D$  from (1)). For simplicity,  
 416 we assumed that  $d \leq D \leq C \cdot d$  for  $C \geq 1$  in (1) in our theoretical bounds. This is without loss  
 417 of generality, as the analysis in the previous section applies to the case where  $D \leq d$  as well.  
 418

of generality by scaling. In practice, we observe that the ratio of distances  $C := D/d$  is always clustered around one. For example, if we use “SFR-Embedding-Mistral” to provide the distance  $D$ , and “bge-micro-v2” to provide the distance  $d$ , then for HotpotQA, we empirically found that 99.9% of  $10^5$  randomly sampled pairs satisfy  $0.6 \leq C \leq 1.5$ . We observed the same qualitative behavior for our other datasets; see Figure 6 in Appendix E.

## 437 4.2 APPLICATION TO A LLM-BASED LISTWISE RERANKER

439 Following the method proposed by Sun et al. (2023), recently, there has been a trend to use LLMs to  
 440 re-rank passages. Though the score output by a re-ranker does not meet the definition of a metric,  
 441 our algorithm still works in this scenario. We prompt *Gemini-2.0-Flash* to re-rank different passages  
 442 based on their relevance to a search query. We slightly modify the search algorithm (Algorithm 4  
 443 in Appendix), as now the re-ranker only returns an order rather than independent relevance scores.  
 444 Since querying proprietary models like *Gemini-2.0-Flash* is expensive, we only use 500 queries  
 445 randomly sampled from the query sets. The averaged results for all 6 data sets are in Figure 2. The  
 446 results on individual dataset and other experimental details are in Appendix E. We can observe that  
 447 our bi-metric framework yields good results in this setting. Our method achieves higher NDCG@10  
 448 scores while sending fewer passages to the re-ranker. (The slight perturbation near the end of the  
 449 curves is because of the LLM’s occasional mistakes in judging the order of different passages.)



450 Figure 2: Average results for 6 BEIR Retrieval datasets. The x-axis is the number  
 451 of passages sent to the reranker. The y-axis is the NDCG@10 score. The cheap distance  
 452 function is provided by “bge-micro-v2”, the  
 453 expensive distance comparator is “Gemini-  
 454 2.0-Flash”, and the nearest neighbor search  
 455 algorithm used is DiskANN.

## 460 5 CONCLUSION

461 We presented a new framework for designing nearest neighbor algorithms that use two metrics: a  
 462 *ground truth* metric  $D$  that defines the true nearest neighbors, and a *proxy* metric  $d$  which provides  
 463 a cheap but imperfect approximation to the ground truth. Our theoretical results show that, as long  
 464 as  $d$  approximates  $D$  up to some constant  $C > 1$ , a nearest neighbor data structure constructed  
 465 using the proxy metric  $d$  can return nearest neighbors with respect to  $D$  up to arbitrarily small  
 466 approximation  $1 + \varepsilon$  in sub-linear time, as long as the ground truth metric  $D$  is used during the query  
 467 answering phase. This improves over an approximation of  $C$  offered by the standard re-ranking  
 468 approach, which retrieves  $k$  nearest neighbors with respect to  $d$ , and then scans them to retrieve the  
 469 true nearest neighbor with respect to  $D$ . Experimentally, we show that our method offers an improved  
 470 accuracy-efficiency tradeoff in settings where  $d$  and  $D$  are computed using embeddings or LLMs of  
 471 vastly different complexities, for BEIR text retrieval benchmarks.

472 Our framework requires that the (cheap) proxy metric  $d$  provides a “reasonable” approximation to  
 473 the (expensive) ground-truth metric  $D$ . The practical effectiveness of our approach, as validated by  
 474 our empirical results on the BEIR benchmark, suggests that such related metrics are readily available  
 475 for real-world datasets. However, the framework’s performance may degrade if the proxy metric is a  
 476 poor approximation of the ground truth. We note that this is an inherent limitation of working with a  
 477 proxy metric, since in the extreme case  $d$  might provide no useful information about  $D$ . However,  
 478 our theorems always guarantees a  $1 + \varepsilon$  approximate solution for any constant  $C$ , with query time  
 479 depending on  $C$ .

480 Our results hold only for graph-based nearest neighbor data structures, and not for other algorithms  
 481 such as LSH. We show that this is a fundamental limitation of LSH itself: in Appendix F, we  
 482 theoretically show that LSH-type algorithms cannot take advantage of a proxy metric.

483 Finally, we recognize that adapting the framework to new domains may require some implementation-  
 484 specific adjustments. For example, when applying our method to an LLM-based listwise reranker, we  
 485 had to modify the search algorithm to accommodate a relative ordering instead of a strict distance  
 486 score. We believe this is a testament to flexibility offered by our framework.

486 REFERENCES  
487

488 Taylor AI. <https://huggingface.co/taylorai/bge-micro-v2>, 2023. URL <https://huggingface.co/TaylorAI/bge-micro-v2>.

489

490 Alexandr Andoni, Piotr Indyk, and Ilya Razenshteyn. Approximate nearest neighbor search in high  
491 dimensions. In *Proceedings of the International Congress of Mathematicians: Rio de Janeiro  
492 2018*, pp. 3287–3318. World Scientific, 2018.

493

494 Martin Aumüller, Erik Bernhardsson, and Alexander Faithfull. Ann-benchmarks: A bench-  
495 marking tool for approximate nearest neighbor algorithms. *Information Systems*, 87:101374,  
496 2020. ISSN 0306-4379. doi: <https://doi.org/10.1016/j.is.2019.02.006>. URL <https://www.sciencedirect.com/science/article/pii/S0306437918303685>.

497

498 Payal Bajaj, Daniel Campos, Nick Craswell, Li Deng, Jianfeng Gao, Xiaodong Liu, Rangan Ma-  
499 jumder, Andrew McNamara, Bhaskar Mitra, Tri Nguyen, Mir Rosenberg, Xia Song, Alina Stoica,  
500 Saurabh Tiwary, and Tong Wang. Ms marco: A human generated machine reading comprehension  
501 dataset, 2018.

502

503 MohammadHossein Bateni, Prathamesh Dharangutte, Rajesh Jayaram, and Chen Wang. Metric  
504 clustering and MST with strong and weak distance oracles. *Conference on Learning Theory*, 2024.  
URL <https://doi.org/10.48550/arXiv.2310.15863>.

505

506 Alina Beygelzimer, Sham Kakade, and John Langford. Cover trees for nearest neighbor. In *Proceed-  
507 ings of the 23rd international conference on Machine learning*, pp. 97–104, 2006.

508

509 Sebastian Borgeaud, Arthur Mensch, Jordan Hoffmann, Trevor Cai, Eliza Rutherford, Katie Millican,  
510 George Bm Van Den Driessche, Jean-Baptiste Lespiau, Bogdan Damoc, Aidan Clark, et al.  
511 Improving language models by retrieving from trillions of tokens. In *International conference on  
machine learning*, pp. 2206–2240. PMLR, 2022.

512

513 Patrick Chen, Wei-Cheng Chang, Jyun-Yu Jiang, Hsiang-Fu Yu, Inderjit Dhillon, and Cho-Jui Hsieh.  
514 Finger: Fast inference for graph-based approximate nearest neighbor search. In *Proceedings of the  
ACM Web Conference 2023*, pp. 3225–3235, 2023.

515

516 Kenneth L Clarkson et al. Nearest-neighbor searching and metric space dimensions. *Nearest-neighbor  
517 methods for learning and vision: theory and practice*, pp. 15–59, 2006.

518

519 Thomas Diggelmann, Jordan Boyd-Graber, Jannis Bulian, Massimiliano Ciaramita, and Markus  
520 Leippold. Climate-fever: A dataset for verification of real-world climate claims, 2020.

521

522 Cong Fu, Chao Xiang, Changxu Wang, and Deng Cai. Nsg : Navigating spread-out graph for  
523 approximate nearest neighbor search. <https://github.com/ZJULearning/nsg>, 2019a.

524

525 Cong Fu, Chao Xiang, Changxu Wang, and Deng Cai. Fast approximate nearest neighbor search with  
526 the navigating spreading-out graph. *Proceedings of the VLDB Endowment*, 12(5):461–474, 2019b.

527

528 Luyu Gao, Zhuyun Dai, and Jamie Callan. Rethink training of bert rerankers in multi-stage retrieval  
529 pipeline. In *Advances in Information Retrieval: 43rd European Conference on IR Research, ECIR  
530 2021, Virtual Event, March 28–April 1, 2021, Proceedings, Part II 43*, pp. 280–286. Springer,  
531 2021a.

532

533 Tianyu Gao, Xingcheng Yao, and Danqi Chen. Simcse: Simple contrastive learning of sentence  
534 embeddings. In *2021 Conference on Empirical Methods in Natural Language Processing, EMNLP  
535 2021*, pp. 6894–6910. Association for Computational Linguistics (ACL), 2021b.

536

537 Anupam Gupta, Robert Krauthgamer, and James R. Lee. Bounded geometries, fractals, and low-  
538 distortion embeddings. In *44th Symposium on Foundations of Computer Science (FOCS 2003),  
539 11–14 October 2003, Cambridge, MA, USA, Proceedings*, pp. 534–543. IEEE Computer Society,  
2003. doi: 10.1109/SFCS.2003.1238226. URL <https://doi.org/10.1109/SFCS.2003.1238226>.

540

541 Sariel Har-Peled and Nirman Kumar. Approximate nearest neighbor search for low-dimensional  
542 queries. *SIAM J. Comput.*, 42(1):138–159, 2013. doi: 10.1137/110852711. URL <https://doi.org/10.1137/110852711>.

540 Ben Harwood and Tom Drummond. Fanng: Fast approximate nearest neighbour graphs. In *Proceedings*  
 541 *of the IEEE Conference on Computer Vision and Pattern Recognition*, pp. 5713–5722,  
 542 2016.

543 Faegheh Hasibi, Fedor Nikolaev, Chenyan Xiong, Krisztian Balog, Svein Erik Bratsberg, Alexander  
 544 Kotov, and Jamie Callan. Dbpedia-entity v2: A test collection for entity search. In *Proceedings*  
 545 *of the 40th International ACM SIGIR Conference on Research and Development in Information*  
 546 *Retrieval, SIGIR '17*, pp. 1265–1268, New York, NY, USA, 2017. Association for Computing  
 547 Machinery. ISBN 9781450350228. doi: 10.1145/3077136.3080751. URL <https://doi.org/10.1145/3077136.3080751>.

548 550 Piotr Indyk and Assaf Naor. Nearest-neighbor-preserving embeddings. *ACM Trans. Algorithms*, 3(3):  
 551 31, 2007. doi: 10.1145/1273340.1273347. URL <https://doi.org/10.1145/1273340.1273347>.

552 553 Piotr Indyk and Hsueh-Yi Wang. Worst-case performance of popular approximate nearest neighbor  
 554 search implementations: Guarantees and limitations. In A. Oh, T. Neumann,  
 555 A. Globerson, K. Saenko, M. Hardt, and S. Levine (eds.), *Advances in Neural Information  
 556 Processing Systems*, volume 36, pp. 66239–66256. Curran Associates, Inc.,  
 557 2023. URL [https://proceedings.neurips.cc/paper\\_files/paper/2023/file/d0ac28b79816b51124fcc804b2496a36-Paper-Conference.pdf](https://proceedings.neurips.cc/paper_files/paper/2023/file/d0ac28b79816b51124fcc804b2496a36-Paper-Conference.pdf).

558 560 Kalervo Järvelin and Jaana Kekäläinen. Cumulated gain-based evaluation of ir techniques. *ACM  
 561 Trans. Inf. Syst.*, 20(4):422–446, oct 2002. ISSN 1046-8188. doi: 10.1145/582415.582418. URL  
 562 <https://doi.org/10.1145/582415.582418>.

563 565 Suhas Jayaram Subramanya, Fnu Devvrit, Harsha Vardhan Simhadri, Ravishankar Krishnawamy, and  
 566 Rohan Kadekodi. Diskann: Fast accurate billion-point nearest neighbor search on a single node.  
 567 *Advances in Neural Information Processing Systems*, 32, 2019.

568 569 Suhas Jayaram Subramanya, Fnu Devvrit, Harsha Vardhan Simhadri, Ravishankar Krishnawamy, and  
 570 Rohan Kadekodi. Diskann. <https://github.com/microsoft/DiskANN>, 2023.

571 572 Herve Jegou, Matthijs Douze, and Cordelia Schmid. Product quantization for nearest neighbor search.  
 573 *IEEE transactions on pattern analysis and machine intelligence*, 33(1):117–128, 2010.

574 575 Herve Jegou, Matthijs Douze, and Cordelia Schmid. Product quantization for nearest neighbor search.  
 576 *IEEE Transactions on Pattern Analysis and Machine Intelligence*, 33(1):117–128, 2011. doi:  
 577 10.1109/TPAMI.2010.57.

578 580 Vladimir Karpukhin, Barlas Oguz, Sewon Min, Patrick Lewis, Ledell Wu, Sergey Edunov, Danqi  
 579 Chen, and Wen-tau Yih. Dense passage retrieval for open-domain question answering. In Bonnie  
 581 Webber, Trevor Cohn, Yulan He, and Yang Liu (eds.), *Proceedings of the 2020 Conference on  
 582 Empirical Methods in Natural Language Processing (EMNLP)*, pp. 6769–6781, Online, November  
 583 2020. Association for Computational Linguistics. doi: 10.18653/v1/2020.emnlp-main.550. URL  
 584 <https://aclanthology.org/2020.emnlp-main.550>.

585 587 Robert Krauthgamer and James R. Lee. Navigating nets: simple algorithms for proximity search.  
 588 In J. Ian Munro (ed.), *Proceedings of the Fifteenth Annual ACM-SIAM Symposium on Discrete  
 589 Algorithms, SODA 2004, New Orleans, Louisiana, USA, January 11-14, 2004*, pp. 798–807. SIAM,  
 590 2004a. URL <http://dl.acm.org/citation.cfm?id=982792.982913>.

591 593 Robert Krauthgamer and James R. Lee. The black-box complexity of nearest neighbor search. In  
 594 *International Colloquium on Automata, Languages, and Programming*, pp. 858–869. Springer,  
 595 2004b.

596 598 Tom Kwiatkowski, Jennimaria Palomaki, Olivia Redfield, Michael Collins, Ankur Parikh, Chris  
 599 Alberti, Danielle Epstein, Illia Polosukhin, Jacob Devlin, Kenton Lee, Kristina Toutanova, Llion  
 600 Jones, Matthew Kelcey, Ming-Wei Chang, Andrew M. Dai, Jakob Uszkoreit, Quoc Le, and Slav  
 601 Petrov. Natural questions: A benchmark for question answering research. *Transactions of the  
 602 Association for Computational Linguistics*, 7:452–466, 2019. doi: 10.1162/tacl\_a\_00276. URL  
 603 <https://aclanthology.org/Q19-1026>.

594 Zehan Li, Xin Zhang, Yanzhao Zhang, Dingkun Long, Pengjun Xie, and Meishan Zhang. Towards  
 595 general text embeddings with multi-stage contrastive learning. *arXiv preprint arXiv:2308.03281*,  
 596 2023.

597 Tie-Yan Liu et al. Learning to rank for information retrieval. *Foundations and Trends® in Information  
 598 Retrieval*, 3(3):225–331, 2009.

600 Weiwen Liu, Yunjia Xi, Jiarui Qin, Fei Sun, Bo Chen, Weinan Zhang, Rui Zhang, and Ruiming  
 601 Tang. Neural re-ranking in multi-stage recommender systems: A review. *arXiv preprint  
 602 arXiv:2202.06602*, 2022.

603 Yu A Malkov and Dmitry A Yashunin. Efficient and robust approximate nearest neighbor search using  
 604 hierarchical navigable small world graphs. *IEEE transactions on pattern analysis and machine  
 605 intelligence*, 42(4):824–836, 2018.

606 Irina Matveeva, Chris Burges, Timo Burkard, Andy Laucius, and Leon Wong. High accuracy  
 607 retrieval with multiple nested ranker. In *Proceedings of the 29th annual international ACM SIGIR  
 608 conference on Research and development in information retrieval*, pp. 437–444, 2006.

609 Rui Meng, Ye Liu, Shafiq Rayhan Joty, Caiming Xiong, Yingbo Zhou, and Semih Yavuz. Sfr-  
 610 embedding-mistral:enhance text retrieval with transfer learning. Salesforce AI Research Blog, 2024.  
 611 URL <https://blog.salesforceairresearch.com/sfr-embedded-mistral/>.

612 Stanislav Morozov and Artem Babenko. Relevance proximity graphs for fast relevance retrieval.  
 613 *arXiv preprint arXiv:1908.06887*, 2019.

614 Benjamin Moseley, Sergei Vassilvtiskii, and Yuyan Wang. Hierarchical clustering in general metric  
 615 spaces using approximate nearest neighbors. In *International Conference on Artificial Intelligence  
 616 and Statistics*, pp. 2440–2448. PMLR, 2021.

617 Shyam Narayanan, Sandeep Silwal, Piotr Indyk, and Or Zamir. Randomized dimensionality reduction  
 618 for facility location and single-linkage clustering. In Marina Meila and Tong Zhang (eds.),  
 619 *Proceedings of the 38th International Conference on Machine Learning, ICML 2021, 18-24 July  
 620 2021, Virtual Event*, volume 139 of *Proceedings of Machine Learning Research*, pp. 7948–7957.  
 621 PMLR, 2021. URL <http://proceedings.mlr.press/v139/narayanan21b.html>.

622 Arvind Neelakantan, Tao Xu, Raul Puri, Alec Radford, Jesse Michael Han, Jerry Tworek, Qiming  
 623 Yuan, Nikolas Tezak, Jong Wook Kim, Chris Hallacy, Johannes Heidecke, Pranav Shyam, Boris  
 624 Power, Tyna Eloundou Nekoul, Girish Sastry, Gretchen Krueger, David Schnurr, Felipe Petroski  
 625 Such, Kenny Hsu, Madeleine Thompson, Tabarak Khan, Toki Sherbakov, Joanne Jang, Peter  
 626 Welinder, and Lilian Weng. Text and code embeddings by contrastive pre-training, 2022.

627 Rodrigo Nogueira and Kyunghyun Cho. Passage re-ranking with bert, 2020.

628 Rodrigo Nogueira, Zhiying Jiang, Ronak Pradeep, and Jimmy Lin. Document ranking with a pre-  
 629 trained sequence-to-sequence model. In *Findings of the Association for Computational Linguistics:  
 630 EMNLP 2020*, pp. 708–718, 2020.

631 Sandeep Silwal, Sara Ahmadian, Andrew Nystrom, Andrew McCallum, Deepak Ramachandran, and  
 632 Seyed Mehran Kazemi. Kwikbucks: Correlation clustering with cheap-weak and expensive-strong  
 633 signals. In *The Eleventh International Conference on Learning Representations, ICLR 2023, Kigali,  
 634 Rwanda, May 1-5, 2023*. OpenReview.net, 2023. URL <https://openreview.net/forum?id=p0JSSa1AuV>.

635 Weiwei Sun, Lingyong Yan, Xinyu Ma, Shuaiqiang Wang, Pengjie Ren, Zhumin Chen, Dawei Yin,  
 636 and Zhaochun Ren. Is chatgpt good at search? investigating large language models as re-ranking  
 637 agents. *arXiv preprint arXiv:2304.09542*, 2023.

638 Nandan Thakur, Nils Reimers, Andreas Rücklé, Abhishek Srivastava, and Iryna Gurevych. BEIR: A  
 639 heterogeneous benchmark for zero-shot evaluation of information retrieval models. In *Thirty-fifth  
 640 Conference on Neural Information Processing Systems Datasets and Benchmarks Track (Round 2)*,  
 641 2021. URL <https://openreview.net/forum?id=wCu6T5xFjeJ>.

648 James Thorne, Andreas Vlachos, Christos Christodoulopoulos, and Arpit Mittal. FEVER: a large-  
 649 scale dataset for fact extraction and VERification. In Marilyn Walker, Heng Ji, and Amanda Stent  
 650 (eds.), *Proceedings of the 2018 Conference of the North American Chapter of the Association*  
 651 *for Computational Linguistics: Human Language Technologies, Volume 1 (Long Papers)*, pp.  
 652 809–819, New Orleans, Louisiana, June 2018. Association for Computational Linguistics. doi:  
 653 10.18653/v1/N18-1074. URL <https://aclanthology.org/N18-1074>.

654 Liang Wang, Nan Yang, Xiaolong Huang, Binxing Jiao, Linjun Yang, Dixin Jiang, Rangan Majumder,  
 655 and Furu Wei. Text embeddings by weakly-supervised contrastive pre-training, 2024.

656 Mengzhao Wang, Xiaoliang Xu, Qiang Yue, and Yuxiang Wang. A comprehensive survey and  
 657 experimental comparison of graph-based approximate nearest neighbor search. *arXiv preprint*  
 658 *arXiv:2101.12631*, 2021.

659 Shitao Xiao, Zheng Liu, Peitian Zhang, and Niklas Muennighoff. C-pack: Packaged resources to  
 660 advance general chinese embedding, 2023.

661 Zhilin Yang, Peng Qi, Saizheng Zhang, Yoshua Bengio, William Cohen, Ruslan Salakhutdinov, and  
 662 Christopher D. Manning. HotpotQA: A dataset for diverse, explainable multi-hop question answer-  
 663 ing. In Ellen Riloff, David Chiang, Julia Hockenmaier, and Jun’ichi Tsujii (eds.), *Proceedings*  
 664 *of the 2018 Conference on Empirical Methods in Natural Language Processing*, pp. 2369–2380,  
 665 Brussels, Belgium, October–November 2018. Association for Computational Linguistics. doi:  
 666 10.18653/v1/D18-1259. URL <https://aclanthology.org/D18-1259>.

667 Zhun Zhong, Liang Zheng, Donglin Cao, and Shaozi Li. Re-ranking person re-identification with  
 668 k-reciprocal encoding. In *Proceedings of the IEEE conference on computer vision and pattern*  
 669 *recognition*, pp. 1318–1327, 2017.

670

671

672

673

674

675

676

677

678

679

680

681

682

683

684

685

686

687

688

689

690

691

692

693

694

695

696

697

698

699

700

701

702 A FURTHER RELATED WORKS  
703

704 **Graph-based algorithms for similarity search** The algorithms studied in this paper rely on  
705 graph-based data structures for (approximate) nearest neighbor search. Such data structures work  
706 for general metrics, which, during the pre-processing, are approximated by carefully constructed  
707 graphs. Given the graph and the query point, the query answering procedure greedily searches the  
708 graph to identify the nearest neighbors. Graph-based algorithms have been extensively studied both  
709 in theory Krauthgamer & Lee (2004a); Beygelzimer et al. (2006) and in practice Fu et al. (2019b);  
710 Jayaram Subramanya et al. (2019); Malkov & Yashunin (2018); Harwood & Drummond (2016).  
711 See Clarkson et al. (2006); Wang et al. (2021) for an overview of these lines of research.

712 **Theorem A.1** (Indyk & Xu (2023)). *Given a dataset  $X$ ,  $\alpha \geq 1$ , and fixed metric  $d$  the slow  
713 preprocessing DiskANN algorithm (Algorithm 4 in Indyk & Xu (2023)) outputs a  $\alpha$ -shortcut reachi-  
714 bility graph  $G$  on  $X$  as defined in Definition 3.1 (under metric  $d$ ). The space complexity of  $G$  is  
715  $n \cdot \alpha^{O(\lambda_d)} \log(\Delta_d)$ .*

718 **Algorithm 1** GreedySearch( $q, d, L$ )

---

719 1: **Input:** Graph index  $G = (X, E)$ , distance function  $d$ , starting point  $s$ , query point  $q$ , queue  
720 length limit  $L$   
721 2: **Output:** visited vertex list  $U$   
722 3:  $A \leftarrow \{s\}$   
723 4:  $U \leftarrow \emptyset$   
724 5: **while**  $A \setminus U \neq \emptyset$  **do**  
725 6:      $v \leftarrow \operatorname{argmin}_{v \in A \setminus U} d(x_v, q)$   
726 7:      $A \leftarrow A \cup \operatorname{Neighbors}(v)$  ▷ Neighbors in  $G$   
727 8:      $U \leftarrow U \cup v$   
728 9:     **if**  $|A| > L$  **then**  
729 10:          $A \leftarrow$  top  $L$  closest vertex to  $q$  in  $A$   
730 11:     sort  $U$  in increasing distance from  $q$   
731 12: **return**  $U$

---

735 B ANALYSIS OF COVER TREE  
736

737 We now analyze Cover Tree under the bi-metric framework. First, some helpful background is  
738 presented below.  
739

740 B.0.1 PRELIMINARIES FOR COVER TREE  
741

742 The notion of a cover is central. We specialize it to the greedy cover used in the Cover Tree  
743 datastructure.  
744

745 **Definition B.1** (Greedy Cover Construction). A  $r$ -cover  $\mathcal{C}$  of a set  $X$  given a metric  $d$  is defined as  
746 follows. Initially  $\mathcal{C} = \emptyset$ . Run the following two steps until  $X$  is empty.

747 1. Pick an arbitrary point  $x \in X$  and remove  $B(x, r) \cap X$  from  $X$ .  
748 2. Add  $x$  to  $\mathcal{C}$ .  
749

750 Note that a cover with radius  $r$  satisfies the following two properties: every point in  $X$  is within  
751 distance  $r$  to some point in  $\mathcal{C}$  (under the same metric  $d'$ ), and all points in  $\mathcal{C}$  are at least distance  $r$   
752 apart from each other.  
753

754 We now introduce the cover tree datastructure of Beygelzimer et al. (2006). For the data structure, we  
755 create a sequence of covers  $\mathcal{C}_{-1}, \mathcal{C}_0, \dots$ . Every  $\mathcal{C}_i$  is a layer in the final Cover Tree  $\mathcal{T}$ .

756

**Algorithm 2** Cover Tree Data structure

757

---

```

1: Input: A set  $X$  of  $n$  points, metric  $d$ , real number  $T \geq 1$ .
2: Output: A tree on  $X$ 
3: procedure COVER-TREE( $d, T$ )
4:   WLOG, all distances between points in  $X$  under  $d$  are in  $(1, \Delta]$  by scaling.
5:    $\mathcal{C}_{-1} = \mathcal{C}_0 = X$ 
6:   Define  $\mathcal{C}_i$  as a  $2^i/T$ -cover of  $\mathcal{C}_{i-1}$  for any  $i > 0$  under metric  $d$ 
7:    $\mathcal{C}_i \subseteq \mathcal{C}_{i-1}$  for all  $i > 0$ .
8:    $t = O(\log(\Delta T))$  ▷  $t$  is the number of levels of  $\mathcal{T}$ 
9:   for  $i = -1$  to  $t$  do
10:     $\mathcal{C}_i$  corresponds to tree nodes of  $\mathcal{T}$  on level  $i$ 
11:    Each  $p \in \mathcal{C}_{i-1} \setminus \mathcal{C}_i$  is connected to exactly one  $p \in \mathcal{C}_i$  such that  $d(p, p') \leq 2^i/T$ 
12:   Return tree  $\mathcal{T}$ 

```

---

769

770

The following result about the space bound of the datastructure is from Beygelzimer et al. (2006) and we to Beygelzimer et al. (2006) for more details about the space bound.

771

**Lemma B.2** (Theorem 1 in Beygelzimer et al. (2006)).  $\mathcal{T}$  takes  $O(n)$  space, regardless of the value of  $r$ .

772

773

*Proof.* We use the *explicit* representation of  $\mathcal{T}$  (as done in Beygelzimer et al. (2006)), where we coalesce all nodes in which the only child is a self-child. The underlying idea is simple: the covers are nested (a smaller scale cover contains all larger scale covers). Thus, a node in the tree has children that also correspond to the same net point. The explicit representation of the tree simply collapses all long paths in the tree (since these correspond to the same net point). Thus, every node in this compressed tree has a parent that represents a different net point and a child that represents a different net point. This can be used to show that there are  $O(n)$  edges in total in the tree, independent of all other parameters.  $\square$

774

775

We note that it is possible to construct the cover tree data structure of Algorithm 2 in time  $2^{O(\lambda_d)} n \log n$ , but it is not important to our discussion Beygelzimer et al. (2006).

776

Now we describe the query procedure. Here, we can query with a metric  $D$  that is possibly different than the metric  $d$  used to create  $\mathcal{T}$  in Algorithm 2.

777

**Algorithm 3** Cover Tree Search

778

---

```

1: Input: Cover tree  $\mathcal{T}$  associated with point set  $X$  , query point  $q$ , metric  $D$ , accuracy  $\varepsilon \in (0, 1)$ .
2: Output: A point  $p \in X$ 
3: procedure COVER-TREE-SEARCH
4:    $t \leftarrow$  number of levels of  $\mathcal{T}$ 
5:    $Q_t \leftarrow \mathcal{C}_t$  ▷ We use the covers that define  $\mathcal{T}$ 
6:    $i \leftarrow t$ 
7:   while  $i \neq -1$  do
8:      $Q = \{p \in \mathcal{C}_{i-1} : p \text{ has a parent in } Q_i\}$ 
9:      $Q_{i-1} = \{p \in Q : D(q, p) \leq D(q, Q) + 2^i\}$ 
10:    if  $D(q, Q_{i-1}) \geq 2^i(1 + 1/\varepsilon)$  then
11:      Exit the while loop.
12:     $i \leftarrow i - 1$ 
13:   Return point  $p \in Q_{i-1}$  that is closest to  $q$  under  $D$ 

```

---

805

806

## B.0.2 THE MAIN THEOREM

807

808

We construct a cover tree  $\mathcal{T}$  using metric  $d$  and  $T$  from Equation 1 in Algorithm 2. Upon a query  $q$ , we search for an approximate nearest neighbor in  $\mathcal{T}$  in Algorithm 3, using metric  $D$  instead. Our main theorem is the following.

810     **Theorem B.3.** Let  $Q_{\text{CoverTree}}(\varepsilon, \Delta_d, \lambda_d) = 2^{O(\lambda_d)} \log(\Delta_d) + (1/\varepsilon)^{O(\lambda_d)}$  denote the query complexity  
 811     of the standard cover tree datastructure, where we set  $T = 1$  in Algorithm 2 and build and search  
 812     using the same metric  $d$ . Now consider two metrics  $d$  and  $D$  satisfying Equation 1. Suppose we  
 813     build a cover tree  $\mathcal{T}$  with metric  $d$  by setting  $T = C$  in Algorithm 2, but search using metric  $D$  in  
 814     Algorithm 3. Then the following holds:

815     1. The space used by  $\mathcal{T}$  is  $O(n)$ .  
 816     2. Running Algorithm 3 using  $D$  finds a  $1 + \varepsilon$  approximate nearest neighbor of  $q$  in the dataset  
 817         $X$  (under metric  $D$ ).  
 818     3. On any query, Algorithm 3 invokes  $D$  at most

819        
$$C^{O(\lambda_d)} \log(\Delta_d) + (C/\varepsilon)^{O(\lambda_d)} = \tilde{O}(Q_{\text{CoverTree}}(\Omega(\varepsilon/C), \Delta_d, \lambda_d)).$$

820        times.

821     Two prove Theorem B.3, we need to: (a) argue correctness and (b) bound the number of times  
 822     Algorithm 3 calls its input metric  $D$ . While both follow from similar analysis as in Beygelzimer  
 823     et al. (2006), it is not in a black-box manner since the metric we used to search  $\mathcal{T}$  in Algorithm 3 is  
 824     different than the metric used to build  $\mathcal{T}$  in Algorithm 2.

825     We begin with a helpful lemma.

826     **Lemma B.4.** For any  $p \in \mathcal{C}_{i-1}$ , the distance between  $p$  and any of its descendants in  $\mathcal{T}$  is bounded  
 827        by  $2^i$  under  $D$ .

828     *Proof.* The proof of the lemma follows from Theorem 2 in Beygelzimer et al. (2006). There,  
 829     it is shown that for any  $p \in \mathcal{C}_{i-1}$  the distance between  $p$  and any descendant  $p'$  is bounded by  
 830         $d(p, p') \leq \sum_{j=-\infty}^{i-1} 2^j/T = 2^i/T$ , implying the lemma after we scale by  $C$  due to Equation 1 (note  
 831        we set  $T = C$  in the construction of  $\mathcal{T}$  in Theorem B.3).  $\square$

832     We now argue accuracy.

833     **Theorem B.5.** Algorithm 3 returns a  $1 + \varepsilon$ -approximate nearest neighbor to query  $q$  under  $D$ .

834     *Proof.* Let  $p^*$  be the true nearest neighbor of query  $q$ . Consider the leaf to root path starting from  $p^*$ .  
 835     We first claim that if  $Q_i$  contains an ancestor of  $p^*$ , then  $Q_{i-1}$  also contains an ancestor  $q_{i-1}$  of  $p^*$ .  
 836     To show this, note that  $D(p^*, q_{i-1}) \leq 2^i$  by Lemma B.4, so we always have

837        
$$D(q, q_{i-1}) \leq D(q, p^*) + D(p^*, q_{i-1}) \leq D(q, Q) + 2^i,$$

838     meaning  $q_{i-1}$  is included in  $Q_{i-1}$ .

839     When we terminate, either we end on a single node, in which case we return  $p^*$  exactly (from the  
 840        above argument), or when  $D(q, Q_{i-1}) \geq 2^i(1 + 1/\varepsilon)$ . In this latter case, we additionally know that

841        
$$D(q, Q_{i-1}) \leq D(q, p^*) + D(p^*, Q_{i-1}) \leq D(q, p^*) + 2^i$$

842     since an ancestor of  $p^*$  is contained in  $Q_{i-1}$  (namely  $q_{i-1}$  from above). But the exit condition implies

843        
$$2^i(1 + 1/\varepsilon) \leq D(q, p^*) + 2^i \implies 2^i \leq \varepsilon D(q, p^*),$$

844     which means

845        
$$D(q, Q_{i-1}) \leq D(q, p^*) + 2^i \leq D(q, p^*) + \varepsilon D(q, p^*) = (1 + \varepsilon)D(q, p^*),$$

846     as desired.  $\square$

847     Finally, we bound the query complexity. The following follows from the arguments in Beygelzimer  
 848     et al. (2006).

849     **Theorem B.6.** The number of calls to  $D$  in Algorithm 3 is bounded by  $C^{O(\lambda_d)} \cdot \log(\Delta_d C) +$   
 850         $(C/\varepsilon)^{O(\lambda_d)}$ .

864 *Proof Sketch.* The bound follows from Beygelzimer et al. (2006) but we briefly outline it here. The  
 865 query complexity is dominated by the size of the sets  $Q_{i-1}$  in Line 9 as the algorithm proceeds. We  
 866 give two ways to bound  $Q_{i-1}$ . Before that, note that the points  $p$  that make up  $Q_{i-1}$  are in a cover  
 867 (under  $d$ ) by the construction of  $\mathcal{T}$ , so they are all separated by distance at least  $\Omega(2^i/C)$  (under  $d$ ).  
 868 Let  $p^*$  be the closest point to  $q$  in  $X$ .  
 869

870 • **Bound 1:** In the iterations where  $D(q, p^*) \leq O(2^i)$ , we have the diameter of  $Q_{i-1}$  under  $D$  is at  
 871 most  $O(2^i)$  as well. This is because an ancestor  $q_{i-1} \in C_{i-1}$  of  $p^*$  is in  $Q$  of line 8 (see proof of  
 872 Theorem B.5), meaning  $D(q, Q) \leq O(2^i)$  due to Lemma B.4. Thus, any point  $p \in Q_{i-1}$  satisfies  
 873  $D(q, p) \leq D(q, Q) + 2^i = O(2^i)$ . From Equation 1, it follows that the diameter of  $Q_{i-1}$  under  
 874  $d$  is also at most  $O(2^i)$ . We know the points in  $Q_{i-1}$  are separated by mutual distance at least  
 875  $\Omega(2^i/C)$  under  $d$ , implying that  $|Q_{i-1}| \leq C^{O(\lambda_d)}$  in this case by a standard packing argument.  
 876 This case can occur at most  $O(\log(\Delta C))$  times, since that is the number of different levels of  $\mathcal{T}$ .  
 877

878 • **Bound 2:** Now consider the case where  $D(q, p^*) \geq \Omega(2^i)$ . In this case, we have that the  
 879 points in  $Q_{i-1}$  have diameter at most  $O(2^i/\varepsilon)$  from  $q$  (under  $D$ ), due to the condition of line  
 880 10. Thus, the diameter is also bounded by  $O(2^i/\varepsilon)$  under  $d$ . By a standard packing argument,  
 881 this means that  $|Q_{i-1}| \leq (C/\varepsilon)^{O(\lambda_d)}$ , since again  $Q_{i-1}$  are mutually separated by distance at  
 882 least  $\Omega(2^i/C)$  under  $d$ . However, our goal is to show that the number of iterations where this  
 883 bound is relevant is at most  $O(\log(1/\varepsilon))$ . Indeed, we have  $D(q, Q_{i-1}) \leq O(2^i/\varepsilon)$ , meaning  
 884  $2^i \geq \Omega(\varepsilon D(q, Q_{i-1})) \geq \Omega(\varepsilon D(q, p^*))$ . Since we are decrementing the index  $i$  and are in the case  
 885 where  $D(q, p^*) \geq \Omega(2^i)$ , this can only happen for  $O(\log(1/\varepsilon))$  different  $i$ 's.  
 886

887 Combining the two bounds proves the theorem.  $\square$   
 888

889 The proof of Theorem B.3 follows from combining Lemmas B.2 and Theorems B.5 and B.6.  
 890

## 891 C OMITTED PROOFS FROM THE MAIN BODY

894 We give the proof of Lemma 3.4

896 *Proof.* Let  $(p, q)$  be a pair of distinct vertices such that  $(p, q) \notin E$ . Then we know that there exists a  
 897  $(p, p') \in E$  such that  $d(p', q) \cdot \alpha \leq d(p, q)$ . From relation (1), we have  $\frac{1}{C} \cdot D(p', q) \cdot \alpha \leq d(p', q) \cdot \alpha \leq$   
 898  $d(p, q) \leq D(p, q)$ , as desired.  $\square$   
 899

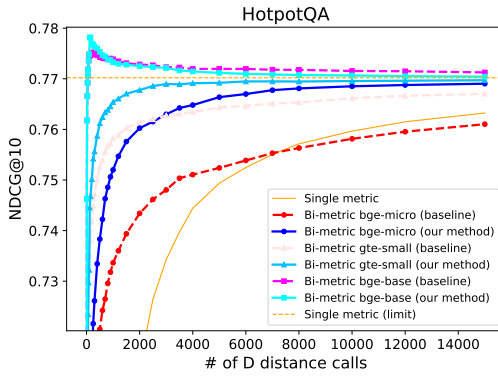
## 901 D ABLATION STUDIES

903 We investigate the impact of different components of our experiments in Section 4. All ablation  
 904 studies are run on HotpotQA dataset as it is one of the largest and most difficult retrieval dataset  
 905 where the performance gaps between different methods are substantial.

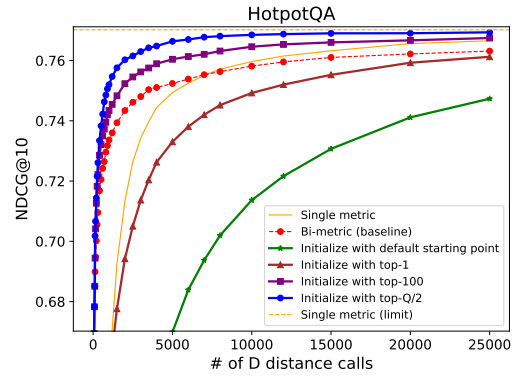
907 **Different model pairs** Fixing the expensive model as “SFR-Embedding-mistral” (Meng et al.,  
 908 2024), we experiment with 2 other cheap models from the BEIR retrieval benchmark: “gte-small”  
 909 Li et al. (2023) and “bge-base” Xiao et al. (2023). These models have different sizes/capabilities,  
 910 summarized in Table 1. For complete results on all 6 BEIR Retrieval datasets for different cheap  
 911 models, we refer to Figures 8, 9, 10, and 11 in Appendix E. Here, we only focus on HotpotQA.

912 From Figure 3, we can observe that the improvement of our method is most substantial when there is  
 913 a large gap between the qualities of the cheap and expensive models. This is not surprising: If the  
 914 cheap model has already provided enough accurate distances, simple re-ranking can easily get to the  
 915 optimal retrieval results with only a few expensive distance calls. Note that even in the latter case,  
 916 our second-stage search method still performs at least as good as re-ranking. Therefore, we believe  
 917 that the ideal scenario for our method is a small and efficient model deployed locally, paired with a  
 remote large model accessed online through API calls to maximize the advantages of our method.

918  
 919 **Varying neighbor search algorithms** We implement our method with another popular empirical  
 920 nearest neighbor search algorithm called NSG (Fu et al., 2019b). We obtain the same qualitative  
 921 behavior as DiskANN, with details given in Section E.



922  
 923  
 924  
 925  
 926  
 927  
 928  
 929  
 930  
 931  
 932  
 933  
 934  
 935 Figure 3: HotpotQA test results for different mod-  
 936 els as the distance proxy. Blue / skyblue / cyan  
 937 curves represent Bi-metric (our method) with bge-  
 938 / gte-small / bge-base models. Red / rose  
 939 / magenta curves represent Bi-metric (baseline)  
 940 with bge-micro / gte-small / bge-base models



935 Figure 4: HotpotQA test results for different  
 936 search initializations for the second-stage search  
 937 of Bi-metric (our method). Blue / purple / brown  
 938 / green curves represent initializing our second-  
 939 stage search with top- $Q/2$ , top-100, top-1, or the  
 940 default vertex.

941  
 942 **Impact of the number of starting points** In the second-stage search of our method, we start from  
 943 multiple points returned by the first-stage search via the cheap distance metric. We investigate how  
 944 varying the starting points for the second-stage search impact the final results. We try four different  
 945 setups:

- 946 • Default: We start a standard nearest neighbor search using metric  $D$  from the default entry point of  
 947 the graph index, which means that we don't use the first stage search.
- 948 • Top- $K$  points retrieved by the first stage search: Suppose our expensive distance calls quota is  $Q$ .  
 949 We start our second search from the top  $K$  points retrieved by the first stage search. We experiment  
 950 with the following different choices of  $K$ :  $K_1 = 1$ ,  $K_{100} = 100$ ,  $K_{Q/2} = \max(100, Q/2)$  (note  
 951  $K_{Q/2}$  is the choice we use in Figure 1).

952  
 953 From Figure 4, we observe that utilizing results from the first-stage search helps the second-stage  
 954 search to find the nearest neighbor quicker. For comparison, we experiment with initializing the  
 955 second-stage search from the default starting point (green), which means that we don't need the  
 956 first-stage search and only use the graph index built from  $d$  (cheap distance function). The DiskANN  
 957 algorithm still manages to improve as the allowed number of  $D$  distance calls increases, but it  
 958 converges the slowest compared to all the other methods.

959  
 960 Using multiple starting points further speeds up the second stage search. If we only start with the  
 961 top-1 point from the first stage search (brown), its NDCG curve is still worse than Bi-metric (baseline),  
 962 red) and Single metric (orange). As we switch to top-100 (purple) or top- $Q/2$  (blue) starting points,  
 963 the NDCG curves increase evidently.

964  
 965 We provide two intuitive explanations for these phenomena. First, the approximation error of the  
 966 cheap distance function doesn't matter that much in the earlier stage of the search, so the first stage  
 967 search with the cheap distance function can quickly get to the true 'local' neighborhood without  
 968 any expensive distance calls, thus saving resources for the second stage search. Second, the ranking  
 969 provided by the cheap distance function is not accurate because of its approximation error, so starting  
 970 from multiple points should give better results than solely starting from the top few, which also  
 971 justifies the advantage of our second-stage search over re-ranking.

972  
 973 **Impact of the first-stage search queue length** In our experiments, we use a very large queue  
 974 length  $L$  for the first-stage search to ensure that the starting point is the closest embedding with

respect to the cheap distance. Here, we perform an ablation study to evaluate how the retrieval quality changes when using smaller queue lengths. On HotpotQA and NQ, we run experiments with varying queue lengths for the first-stage search; see Figure 5. We observe that different values of  $L$  impact the final retrieval quality noticeably on HotpotQA but not much on NQ. Overall, the NDCG curves become stable after  $L = 1000$  for both datasets.

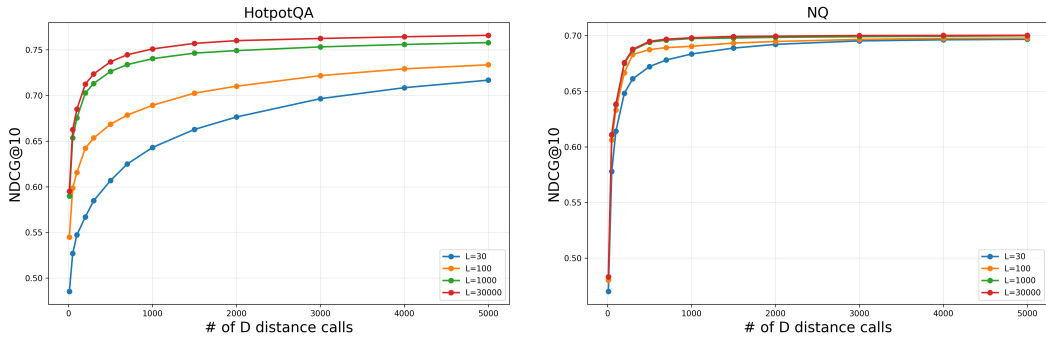


Figure 5: HotpotQA and NQ test results for different first stage queue length  $L = \{30, 100, 1000, 30000\}$

## E COMPLETE EXPERIMENTAL RESULTS

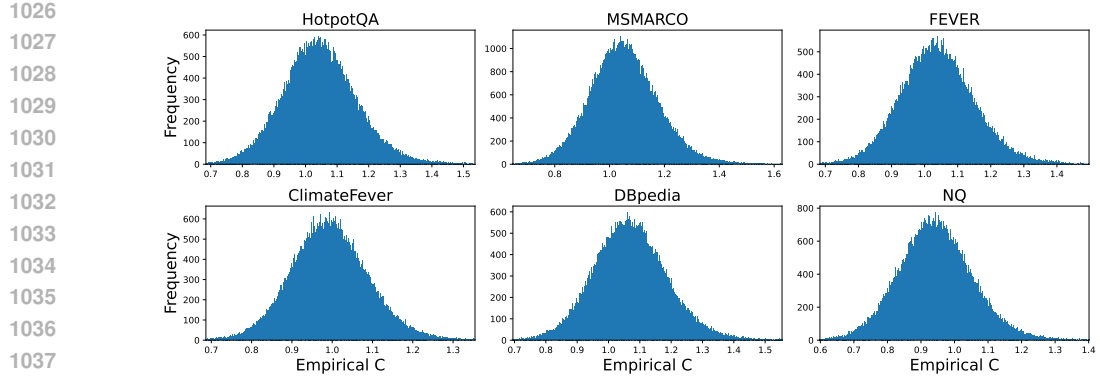
**Parameter choices for Nearest Neighbor Search algorithms** The parameter choices for DiskANN are  $\alpha = 1.2$ ,  $l\_build = 125$ ,  $max\_outdegree = 64$  (the standard choices used in ANN benchmarks Aumüller et al. (2020)). The parameter choices for NSG are the same as the authors’ choices for GIST1M dataset (Jégou et al., 2011):  $K = 400$ ,  $L = 400$ ,  $iter = 12$ ,  $S = 15$ ,  $R = 100$ . NSG also requires building a knn-graph with efanna, where we use the standard parameters:  $L = 60$ ,  $R = 70$ ,  $C = 500$ .

**Empirical Results** We report the empirical results of using different embedding models as distance proxy, using the NSG algorithm, and measuring Recall@10.

1. We report the results of using “bge-micro-v2” as the distance proxy  $d$  and using DiskANN for building the graph index. See Figure 7 for Recall@10 metric plots.
2. We report the results of using “gte-small” as the distance proxy  $d$  and using DiskANN for building the graph index. See Figure 8 for NDCG@10 metric plots and Figure 9 for Recall@10 metric plots.
3. We report the results of using “bge-base-en-v1.5” as the distance proxy  $d$  and using DiskANN for building the graph index. See Figure 10 for NDCG@10 metric plots and Figure 11 for Recall@10 metric plots.
4. We report the results of using “bge-micro-v2” as the distance proxy  $d$  and using NSG for building the graph index. See Figures 12 for NDCG@10 metric plots and 13 for Recall@10 metric plots.

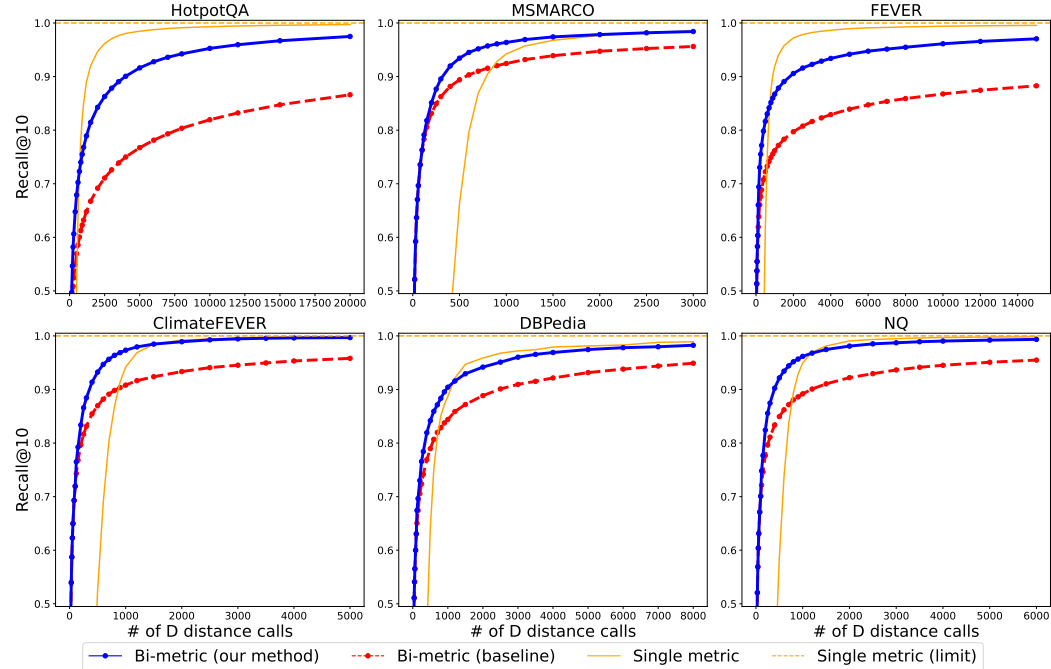
We can see that for all the different cheap distance proxies (“bge-micro-v2” Xiao et al. (2023), “gte-small” Li et al. (2023), “bge-base-en-v1.5” Xiao et al. (2023)) and both nearest neighbor search algorithms (DiskANN Jayaram Subramanya et al. (2019) and NSG Fu et al. (2019b)), our method has better NDCG and Recall results on most datasets. Moreover, naturally the advantage of our method over Bi-metric (baseline) is larger when there is a large gap between the qualities of the cheap distance proxy  $d$  and the ground truth distance metric  $D$ . This makes sense because as their qualities converge, the cheap proxy alone is enough to retrieve the closest points to a query for the expensive metric  $D$ .

We also report the histograms of empirical  $C = d/D$  values using “bge-micro-v2” as the distance proxy  $d$  in Figure 6. For all 6 datasets, the distance ratio  $C = d/D$  concentrates well around 1



1039 Figure 6: Results for 6 BEIR Retrieval datasets. Histograms of  $C = D/d$  values, where we use  
1040 “bge-micro-v2” as the distance proxy  $d$  and “SFR-Embedding-Mistral” as the expensive distance  $D$ .  
1041

1042 **Different nearest neighbor search algorithms** We implement our method with another popular  
1043 empirical nearest neighbor search algorithm called NSG Fu et al. (2019b). We obtain the same  
1044 qualitative behavior as DiskANN. Because the authors’ implementation of NSG only supports  $\ell_2$   
1045 distances, we first normalize all the embeddings and search via  $\ell_2$ . This may cause some performance  
1046 drops. Therefore, we are not comparing the results between the DiskANN and NSG algorithms, but  
1047 only results from different methods, fixing the graph index. In Figure 12 and 13 in the appendix, we  
1048 observe that our method still performs the best compared to Bi-metric (baseline) and single metric in  
1049 most cases, demonstrating that our bi-metric framework can be applied to other graph-based nearest  
1050 neighbor search algorithms as well.



1074 Figure 7: Results for 6 BEIR Retrieval datasets. The x-axis is the number of expensive distance  
1075 function calls. The y-axis is the Recall@10 score. The cheap model is “bge-micro-v2”, the expensive  
1076 model is “SFR-Embedding-Mistral”, and the nearest neighbor search algorithm used is DiskANN.  
1077

1078 **Details of the LLM-based listwise reranking experiment** Here we provide the details for our  
1079 experiments in Section 4.2. Due to the fact that LLMs are better at comparing the relevancy of

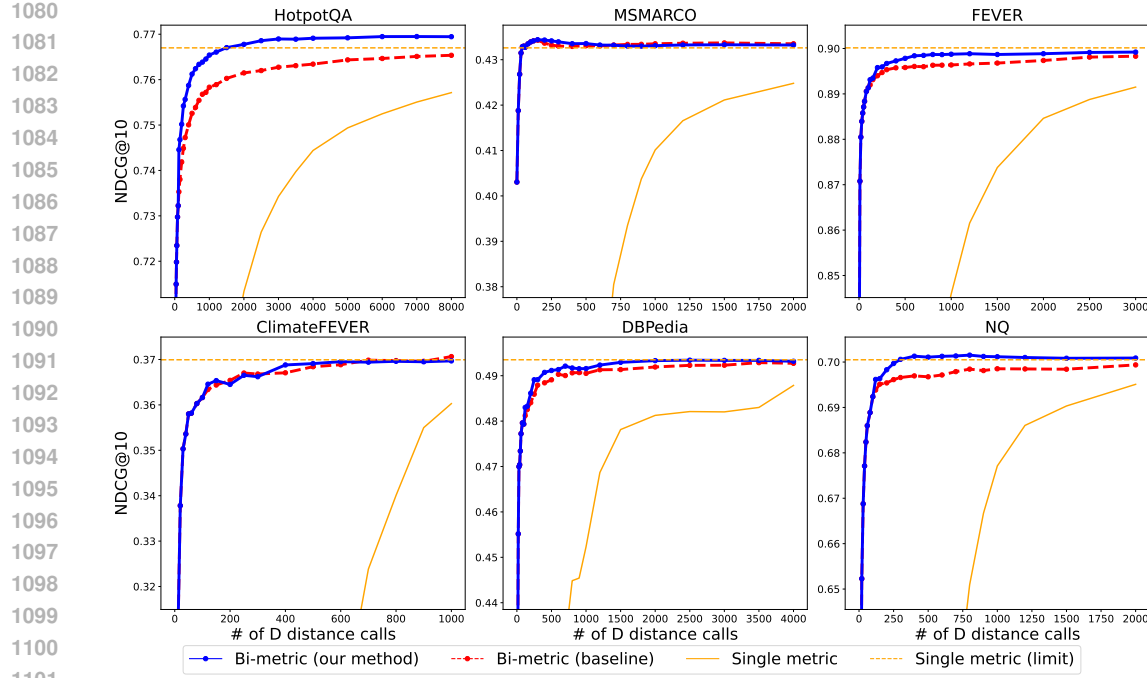


Figure 8: Results for 6 BEIR Retrieval datasets. The x-axis is the number of expensive distance function calls. The y-axis is the NDCG@10 score. The cheap model is “gte-small”, the expensive model is “SFR-Embedding-Mistral”, and the nearest neighbor search algorithm used is DiskANN.

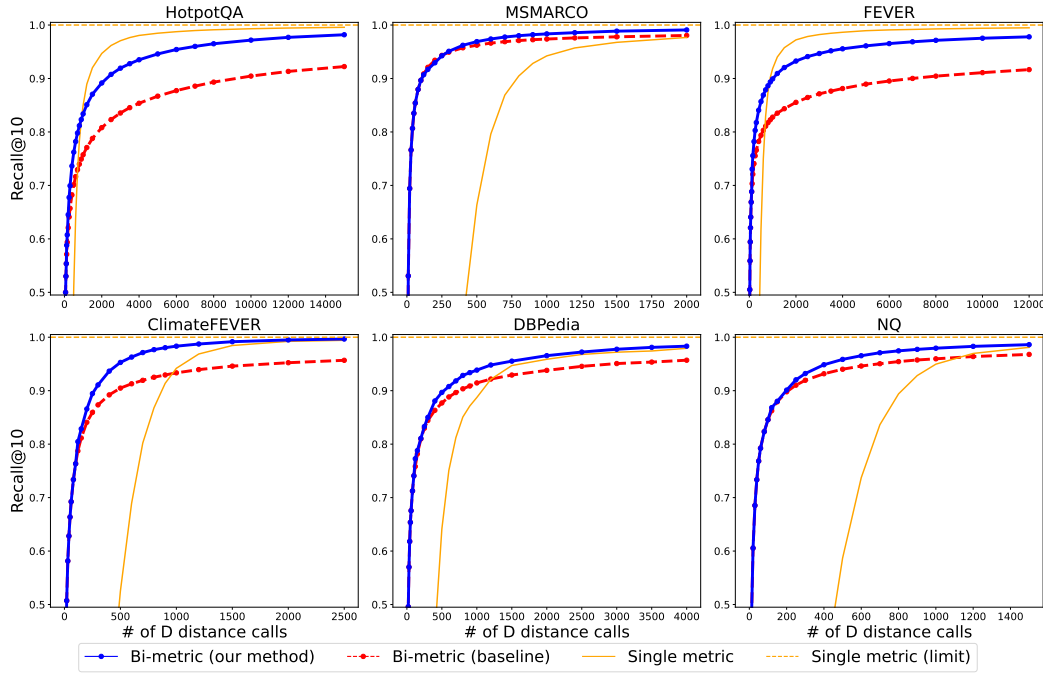


Figure 9: Results for 6 BEIR Retrieval datasets. The x-axis is the number of expensive distance function calls. The y-axis is the Recall@10 score. The cheap model is “gte-small”, the expensive model is “SFR-Embedding-Mistral”, and the nearest neighbor search algorithm used is DiskANN.

different passages than providing independent relevance scores, we need to modify our algorithm to maintain a list of  $L_s$  current best answers. Please see our Algorithm 4. Its difference from Algorithm 1

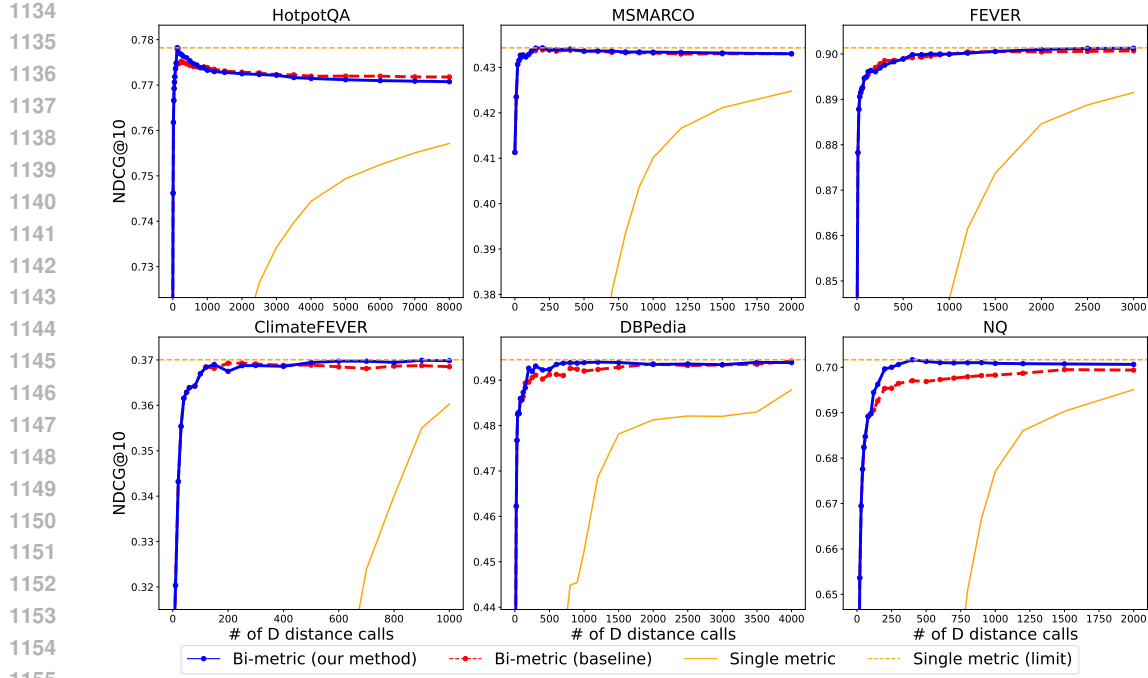


Figure 10: Results for 6 BEIR Retrieval datasets. The x-axis is the number of expensive distance function calls. The y-axis is the NDCG@10 score. The cheap model is “bge-base-en-v1.5”, the expensive model is “SFR-Embedding-Mistral”, and the nearest neighbor search algorithm used is DiskANN.

1161	System	You are RankGPT, an intelligent assistant that can rank answers based on their
1162	Instruction	relevancy to the query. I will provide you with 10 passages, each indicated
1163		by number identifier []. Rank the answers based on their relevance to query:
1164		{query}.
1165		[1] {Passage 1}
1166		[2] {Passage 2}
1167	Messages	...
1168		[10] {Passage 10}
1169		Query: {query}. Rank the 10 passages above based on their relevance to the
1170		query. The passages should be listed in descending order using identifiers. The
1171		most relevant passages should be listed first. The output format should be like
1172		[1] >[2] ... >[10]. Only response the ranking results, do not say any word or
1173		explain.

Table 2: Prompt for “Gemini-2.0-Flash” to rerank passages

is that instead of maintaining a priority queue  $A$ , in Algorithm 4,  $A$  is an ordered list. At each step, we first append all the unseen neighbors of  $v$  to the end of  $A$ , and then perform a sequential reranking in a sliding window way to update the current top passages, similar to the application of listwise rerank in Sun et al. (2023). In the experiment, we set  $L_s = 50$ ,  $w = 10$ . We start our second stage search from  $\max(50, Q/2)$  points retrieved by the first stage search where  $Q$  is quota set to be the maximal number of passages seen by the reranker. Please See Table 2 for our prompt.

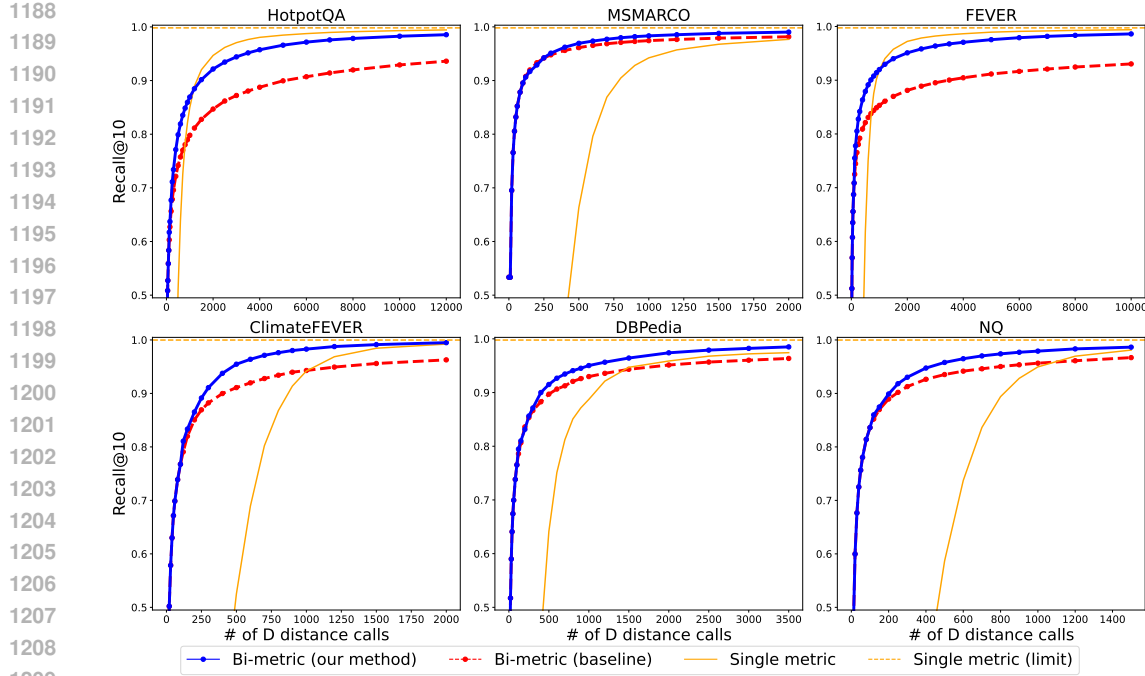


Figure 11: Results for 6 BEIR Retrieval datasets. The x-axis is the number of expensive distance function calls. The y-axis is the Recall@10 score. The cheap model is “bge-base-en-v1.5”, the expensive model is “SFR-Embedding-Mistral”, and the nearest neighbor search algorithm used is DiskANN.

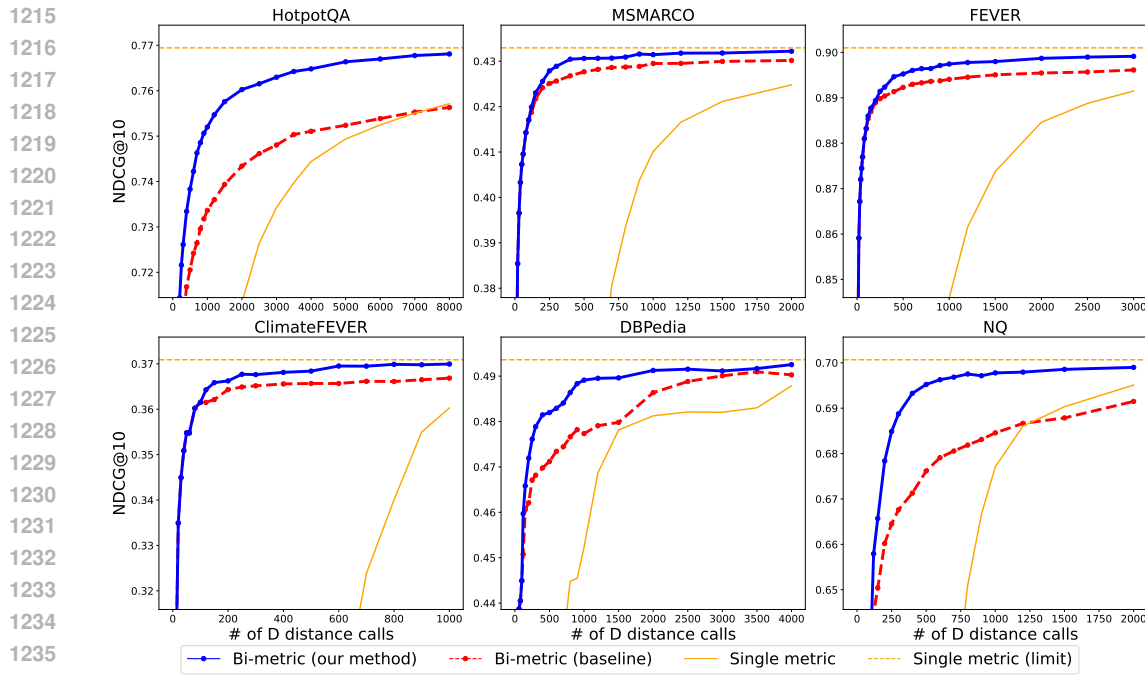


Figure 12: Results for 6 BEIR Retrieval datasets. The x-axis is the number of expensive distance function calls. The y-axis is the NDCG@10 score. The cheap model is “bge-micro-v2”, the expensive model is “SFR-Embedding-Mistral”, and the nearest neighbor search algorithm used is NSG.

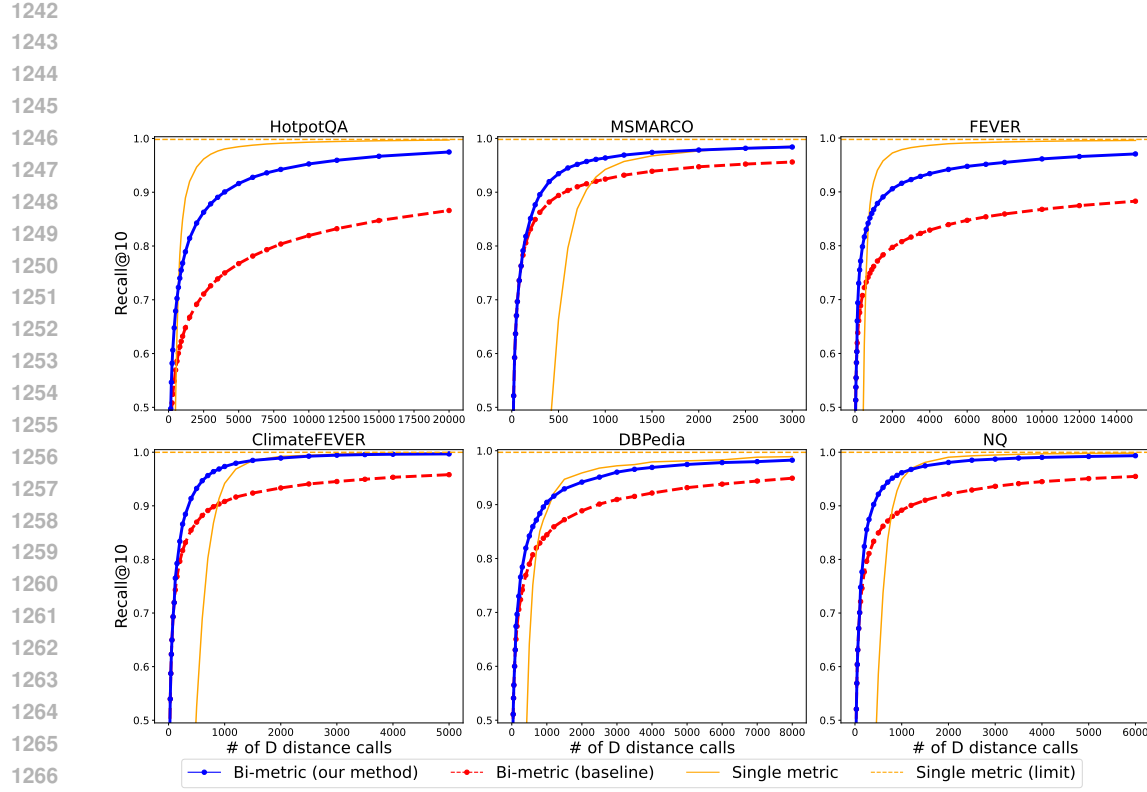


Figure 13: Results for 6 BEIR Retrieval datasets. The x-axis is the number of expensive distance function calls. The y-axis is the Recall@10 score. The cheap model is “bge-micro-v2”, the expensive model is “SFR-Embedding-Mistral”, and the nearest neighbor search algorithm used is NSG.

---

**Algorithm 4** Order-GreedySearch( $q, d$ )

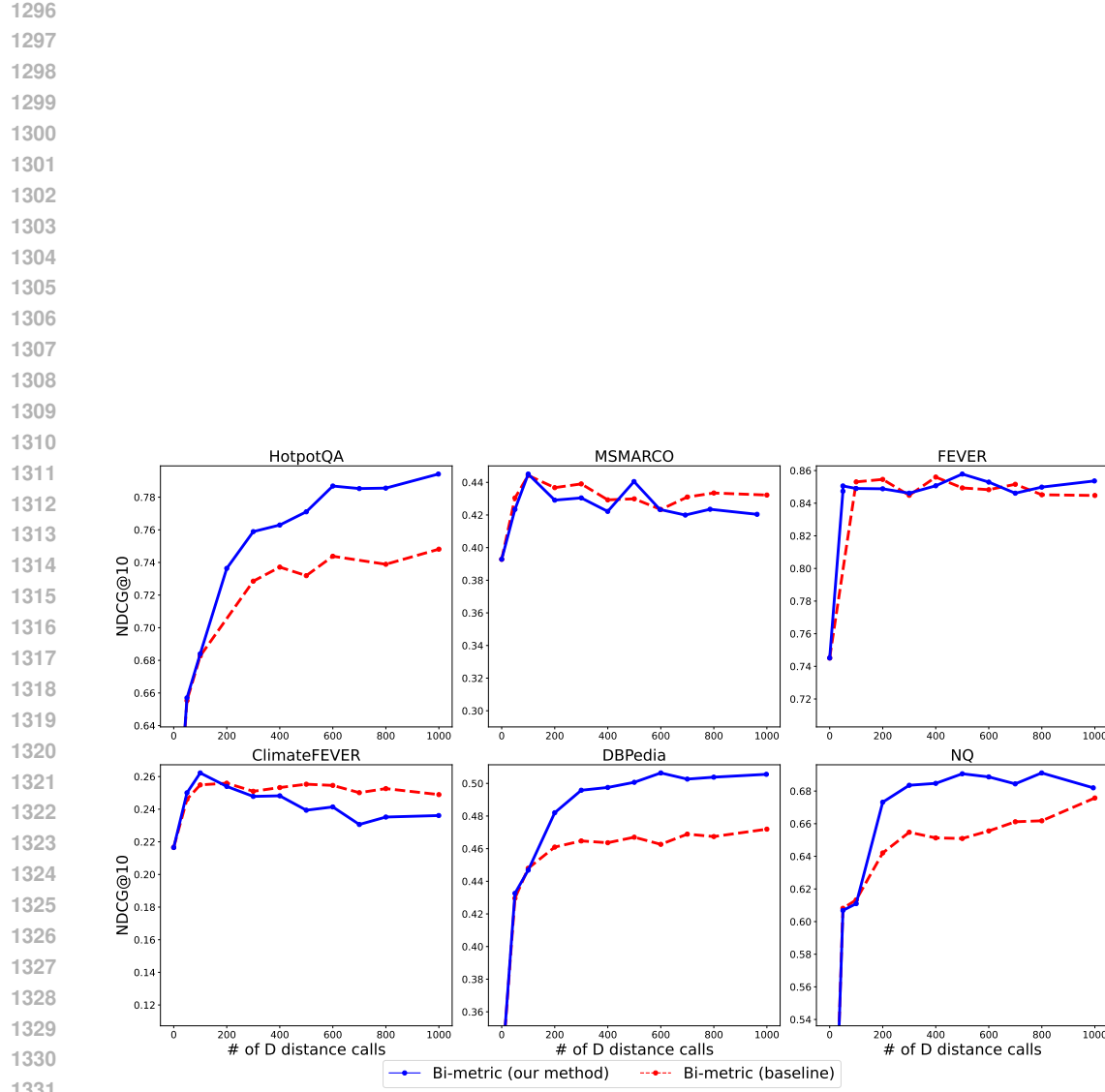
---

```

1: Input: Graph index  $G = (X, E)$ , listwise-reranker  $D$ , starting point  $s$ , query point  $q$ , queue
2: Output: a sorted vertex list  $A$ 
3:  $A \leftarrow \{s\}$  ▷ An ordered list of vertices
4:  $U \leftarrow \emptyset$ 
5: while  $A \setminus U \neq \emptyset$  do
6:    $v \leftarrow$  the first vertex in  $A \setminus U$ 
7:    $U \leftarrow U \cup v$ 
8:   Append  $Neighbors(v) \setminus A$  to the end of  $A$  ▷ Neighbors in  $G$ 
9:   for  $i = |A|$  to 0 step size  $-w/2$  do
10:    Use  $D$  to rerank ( $A[i - w], \dots, A[i]$ )
11:    if  $|A| > L$  then
12:       $A \leftarrow$  the first  $L$  vertices in  $A$ 
13: return  $A$ 

```

---



1332 Figure 14: Results for 6 BEIR Retrieval datasets. The x-axis is the number of passages sent to the  
 1333 reranker. The y-axis is the NDCG@10 score. The cheap distance function is provided by “bge-micro-  
 1334 v2”, the expensive model distance comparator is “Gemini-2.0-Flash”, and the nearest neighbor search  
 1335 algorithm used is DiskANN.

1350 **F DISCUSSION ON LSH**  
 1351

1352 We give a very simple example, showing that the standard locality sensitive hashing (LSH) algorithm  
 1353 can be easily ‘tricked’ in our two distance functions setting, even if the distances approximate each  
 1354 other very well. Thus, locality sensitive hashing cannot be instantiated in the bi-metric framework,  
 1355 demonstrating the power of graph-based approaches. In fact, our construction extends to a broad  
 1356 class of algorithms which ‘overfit’ to the coordinates of the vectors. The intuitive idea is that any  
 1357 algorithm which ‘only looks’ at the coordinates of the query vector during the query phase can be  
 1358 fooled by fixing the coordinates of the query across the two metrics, but changing the coordinates  
 1359 of the input dataset slightly. At the core, LSH, as well as many partition based algorithms, can be  
 1360 abstracted into the following canonical form:

1361 1. Given an input dataset  $X \subset \mathbb{R}^d$ ,  $|X| = n$  and an input metric, output a function  $f : \mathbb{R}^d \rightarrow 2^{[n]}$ .  
 1362 2. Given a query point  $q \in \mathbb{R}^d$ , query  $f(q)$  to return a subset of  $[n]$ .  
 1363 3. Find the nearest neighbor of  $q$  using the input metric among the points in  $X$  whose indices are  
 1364 in  $f(q)$ . We define the running time of  $f$  to be  $O(|f(q)| \cdot T)$ , where  $T$  is the cost to evaluate the  
 1365 metric. For simplicity, we ignore this factor of  $T$  in the subsequent discussion.

1366 The main conceptual difference between the above canonical form and our graph based approach is  
 1367 that the query is used in ‘one shot’ to return the set  $f(q)$  at once. This is problematic when using two  
 1368 distances in our bi-metric framework since  $f(q)$  only depends on  $d$  above (the cheap metric), but we  
 1369 want to find the nearest neighbor with respect to  $D$  (the ground truth metric). In contrast, graph based  
 1370 approaches iteratively and adaptively build such a query set, based on the edges of the index graph  
 1371 and the corresponding search procedure on the graph. The fact that the query set is a function of *both*  
 1372 metrics in graph based search is crucial in avoiding the undesired behavior shown below.

1373 We first note the following trivial observation.

1374 **Observation:** Let  $X, X' \subset \mathbb{R}^d$ ,  $|X| = |X'|$  be two datasets with corresponding metrics  $d$  and  
 1375  $d'$ . Suppose we instantiate the above canonical algorithm on  $X'$  using metric  $d'$  and let  $f'$  be the  
 1376 corresponding query function. Let  $q$  be a query point for the dataset  $X$  and let  $i^*$  be the index of its  
 1377 nearest neighbor in  $X$  with respect to  $d$ . If  $i^* \notin f'(q)$  then we cannot find the nearest neighbor of  $q$   
 1378 in  $X$  by only comparing the distances from  $q$  to the points in  $f'(q)$  (even if we evaluate using metric  
 1379  $d$  on the points in  $f'(q)$ ).

1380 Now lets discuss how the standard LSH algorithms fall in the above canonical description. We need  
 1381 to first specify a family of hash functions  $\mathcal{H}$ . Then for some suitably chosen parameters  $k, L \geq 1$ ,  
 1382 we repeat the following procedure for  $i = 1, \dots, L$  iterations : Independently sample  $k$  functions  
 1383  $h_1^i, \dots, h_k^i \sim \mathcal{H}$  and group the points by putting all  $x$  with the same tuple  $(h_1^i(x), \dots, h_k^i(x))$  together.  
 1384 For a query  $q$ , retrieve all the points in  $X$  with the same tuples  $(h_1^i(q), \dots, h_k^i(q))$  across all  $i$ . This  
 1385 forms the set  $f(q)$ . Usually,  $|f(q)|$  is determined by the choice of  $\mathcal{H}, k, L$  and for different metrics,  
 1386 researchers carefully choose these parameters to optimize for correctness and running time Andoni  
 1387 et al. (2018). We do not need these details in constructing the bad example and they can be abstracted  
 1388 away in our description of the canonical algorithm.

1389 Our simple bad example for LSH is as follows. The dataset is  $X = \{x_1, \dots, x_n\} \subset \mathbb{R}^d$  (for  $d$   
 1390 sufficiently large). It consists of one copy of the first basis vector  $x_1 = e_1$  and  $n - 1$  copies of the  
 1391 sum of the first two basis vectors:  $x_2 = \dots = x_n = e_1 + e_2$ . The ground truth metric  $D$  will be  
 1392 the hamming distance on the vectors in  $X$ . The noisy metric  $d$  will be the hamming distance on the  
 1393 corresponding points of a modified version of  $X$ . The modified dataset  $X' = \{x'_1, \dots, x'_n\}$  is such  
 1394 that  $x'_1$  is just  $x_1$  but we set the last 10 coordinates to all 1’s. For the other  $x'_i$  vectors,  $i \geq 2$ , we keep  
 1395 the same  $x_i$ , but modify the last 5 coordinates to be all 1’s. We have:

1396 

- 1397 •  $d$  approximates  $D$  up to a factor of  $O(1)$ .
- 1398 • The doubling dimensions of both  $X'$  and  $X$  (under  $d$  and  $D$  respectively) are  $O(1)$ .

1399 We let the query vector  $q$  be the all 0’s vector ( $q$  will be all 0’s with respect to  $D$  and  $d$ ). In  $X$ ,  $x_1$   
 1400 is the  $c$ -approximate nearest neighbor to  $q$  for any  $c < 2$ . Note this is a setting where our theorems  
 1401 *guarantee* the performance of graph based algorithms (Theorems 3.3 and B.3), giving meaningful  
 1402 sublinear running time. For the rest of the section, we fix the query  $q = 0$ .

Now consider what happens when we use the standard hamming LSH function ( $\mathcal{H}$  is the set of coordinate projection functions) and build a datastructure  $f'$  using the noisy metric. Intuitively, unless  $k$  and  $L$  are sufficiently large, we cannot even guarantee with good probability that  $1 \in f'(0)$  (note this means that the index of the first point is in the set  $f'(0)$ ). However if we can guarantee that the ‘correct’ answer is in  $f'(0)$ , many irrelevant data points are also very likely to be in  $f'(0)$ , implying  $|f'(0)| = \Omega(n)$ , i.e. the query time is linear and hence not efficient. This is shown below.

**Lemma F.1.** *Suppose  $(k, L)$  such that*

$$\Pr(1 \in f'(0)) \geq 0.01,$$

*i.e. the query is successful with probability at least 1%. With these same parameters, we have  $\mathbb{E}[|f'(0)|] = \Omega(n)$ .*

*Proof.* A simple calculation shows the following (since our hash functions are sampled from coordinate projections):

$$\Pr_{h \sim \mathcal{H}}(h(x'_1) = h(0)) = \frac{d-11}{d} := p_1 \leq \Pr_{h \sim \mathcal{H}}(h(x'_i) = h(0)) = \frac{d-7}{d} := p_2$$

for any other  $i \geq 2$ . If we repeat the hashing  $k$  times, it is clear that the probability that  $(h_1(x'_1), \dots, h_k(x'_1)) = (h_1(0), \dots, h_k(0)) = p_1^k \leq p_2^k$ . Thus, for any choice of  $k$  and  $L$ , we have that for all  $i \geq 2$ ,

$$\Pr(1 \in f'(0)) \leq \Pr(i \in f'(0)).$$

Hence, if  $k, L$  is picked such that  $\Pr(1 \in f'(0)) \geq 0.01$ , it follows that

$$\mathbb{E}[|f'(0)|] = \sum_{i=1}^n \Pr(i \in f'(0)) \geq n \Pr(1 \in f'(0)) \geq \Omega(n),$$

as desired. □

In conclusion, the above lemma shows that unless the set  $f'(q)$  is very large, which leads to a large running time for using LSH, it cannot be successfully used for nearest neighbor search with two metrics, in contrast to our graph based approach. The underlying idea of our bad example clearly generalizes across any reasonable choice of  $\mathcal{H}$ . The proof of the following corollary is identical to that of Lemma F.1.

**Corollary F.2.** *Suppose  $\mathcal{H}$  is a family of functions with domain  $\mathbb{R}^d$  such that  $\Pr_{h \sim \mathcal{H}}(h(x) = h(y))$  is a decreasing function of  $\|x - y\|_2$ . Consider  $X$  and  $X'$  as defined above. Then if  $(k, L)$  are picked such that*

$$\Pr(1 \in f'(0)) \geq 0.01,$$

*i.e. the query is successful with probability at least 1%. With these same parameters, we have  $\mathbb{E}[|f'(0)|] = \Omega(n)$ .*

The hypothesis on  $\mathcal{H}$  in Corollary F.2 is quite natural and is satisfied by many natural choices. For example, the standard Euclidean LSH function class  $\mathcal{H}$  consists of functions of the form  $h_v(x) = \lfloor \langle x, v \rangle / a \rfloor$  where  $v \sim \mathcal{N}(0, 1)$ . A simple calculation shows that  $\Pr_{h \sim \mathcal{H}}(h(x) = h(y)) \propto \|x - y\|_2$  and Corollary F.2 applies.

Upon a closer look, we can even abstract away all the details of LSH and return to the canonical form described in the beginning of the section. All we require for the bad example to hold is that  $\Pr(i \in f'(0))$  is a decreasing function of  $\|x'_i - q\|_2 = \|x'_i\|_2$ .

**Corollary F.3.** *Suppose in our canonical algorithm description that  $f'$  is a function such that for all indices  $1 \leq i \leq n$ ,  $\Pr(i \in f'(0))$  is an decreasing function of  $\|x'_i\|_2$ . If*

$$\Pr(1 \in f'(0)) \geq 0.01,$$

*i.e. the query is successful with probability at least 1%, then we also have  $\mathbb{E}[|f'(0)|] = \Omega(n)$ .*

## G USAGE OF LARGE LANGUAGE MODELS

As mentioned in Section 4.2, we apply an LLM-based reranker in our experiments. We also use LLMs to polish writing.